

Image Sensors and Photodetectors Based on Low-Carbon Footprint Solution-Processed Semiconductors

William Solari, Renjun Liu, Serena N. Erkizan, Alexander R. C. Osypiw, Peter M. Smowton, and Bo Hou*

This mini-review explores the evolution of image sensors, essential electronic components increasingly integrated into daily life. Traditional manufacturing methods for image sensors and photodetectors, employing high carbon footprint techniques like thermal evaporation and chemical vapor deposition, are being replaced by environmentally conscious solution processing. Organic and Colloidal Quantum Dot-based image sensors emerge as promising candidates, aligning with the shift toward solution-based device integration. This review provides insights into the working principles of photodetectors and image sensors, summarizing relevant materials and fabrication approaches. Additionally, it delves into the detailed exploration of pixelated patterning techniques and their potential applications in the realm of solution-processed image sensor fabrication.

1. Introduction

PhotoDetectors (PD) and Image sensors are essential to modern everyday life.^[1,2] They are used in almost every electronic device, from mobile phones to medical imaging to being used in industry to monitor various processes. As such they are an area that is heavily researched across the globe.^[2,3,4] The global focus on research for a long time was on how to lower the pixel size to increase resolution, however, in recent years, there has been a step away from this area and more toward device efficiency, fidelity to color and the attempt to make these devices more “smart”, to be integrated with other devices for various purposes.^[5]

Solution-processed PDs are of particular interest currently, including organic and Colloidal Quantum Dot (QD) based PDs, due to their low carbon footprint and potential for complex device fabrication.^[6,7] This means that the PhotoActive (PA) layer of the


device is either a semiconducting organic molecule that absorbs and emits photons or QDs that do the same. These two materials have different qualities that makes them unique: i) organics have a wide range of different absorption spectra and conductive properties to choose from, which can be controlled by changing atoms and moieties in the molecular chains.^[8,9] ii) QDs have a broad absorption with sharp excitonic absorption bands and a narrowband emission peak due to the quantum confinement effect, which means they interact very strongly with certain energies of photons and electrons, combined with a tuneable bandgap by altering the size or composition of the

particles.^[10,11] As such, both of these materials can be used to achieve different effects in their devices.

The method by which these devices function is that when incident light hits the transparent electrode at the top or bottom of the device, the photons then pass through the device, likely interacting weakly along the way until they reach the PA organic or QD layer. At this point, they are highly absorbed, ideally, by the PA layer. When the photons are absorbed, there is an electron-hole pair generated at the site of the extinction of the photon. This electron-hole pair disassociates immediately (inorganic semiconductors) or is weakly bonded together and diffuses to the junction before splitting into electron and hole (organic semiconductors) to travel to their respective electrodes.^[2,4,11,12] At the electrodes, the electrons and holes flow through the connected circuit in turn generating a photocurrent.

Typically, these devices are crafted using a layer-by-layer approach, incorporating diverse techniques such as spin-coating,^[11] dip coating,^[11,13] inkjet printing,^[11,14,15] thermal evaporation,^[16,17] ElectroPhoretic Deposition (EPD),^[18,19] and transfer printing.^[20] While spin-coating stands as the most prevalent method, alternatives such as thermal evaporation and transfer printing can enhance film production quality. These methods serve as the primary commercially employed strategies for manufacturing solution-processed photodetection devices, be they organic or QD-based. This review will specifically focus on organic semiconductors (briefly) and comprehensively cover colloidal quantum dots. Other materials, such as silicon,^[21] III-V epitaxial semiconductors,^[22] perovskites,^[23] graphene,^[24] or transition metal chalcogenide (TMC),^[25] have been thoroughly examined in prior reviews, and readers seeking additional details can refer to the cited references.

W. Solari, R. Liu, S. N. Erkizan, A. R. C. Osypiw, P. M. Smowton, B. Hou
School of Physics and Astronomy
Cardiff University
The Parade, Cardiff CF24 3AA, UK
E-mail: houb6@cardiff.ac.uk

 The ORCID identification number(s) for the author(s) of this article can be found under <https://doi.org/10.1002/adsr.202400059>

© 2024 The Author(s). Advanced Sensor Research published by Wiley-VCH GmbH. This is an open access article under the terms of the [Creative Commons Attribution](#) License, which permits use, distribution and reproduction in any medium, provided the original work is properly cited.

DOI: 10.1002/adsr.202400059

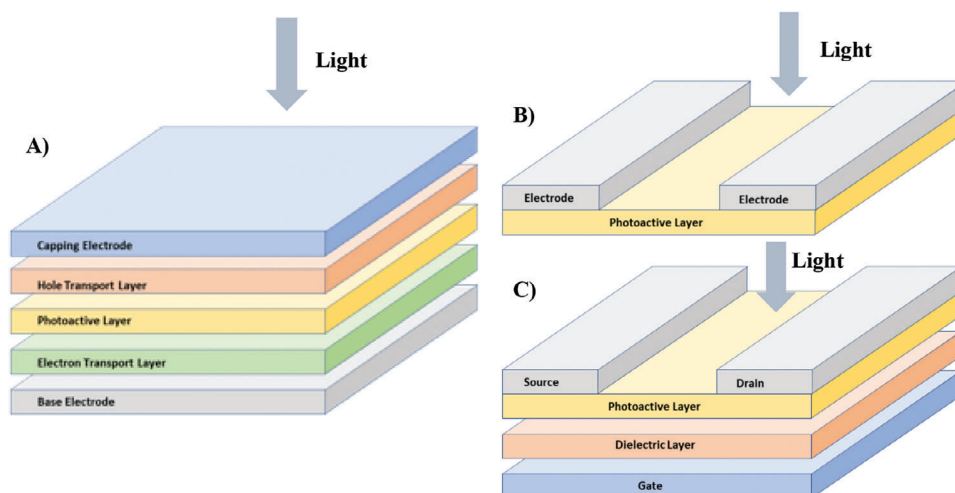


Figure 1. Diagram showing device structure for A) Photodiode, B) Photoconductor, and C) Phototransistor. It is assumed that light is incident from the top of the devices as denoted by the arrows.

1.1. Photodetectors

Photodetection devices tend to fit into one of three different structure categories, PhotoDioDe (PDD), PhotoTransistor (PT), or PhotoConductor (PC) as shown in **Figure 1**.^[26] These structures have certain attributes which can benefit, or hinder devices based on the purpose of the device.

A simple PDD structure typically includes five basic layers, the base electrode, the Hole Transport Layer (HTL), the PA layer, the Electron Transport Layer (ETL), and the capping electrode.^[26] To improve device performance, additional layers can also be added such as charge blocking layers and passivation or encapsulation layers.^[27] The important thing to note with this structure is that the bandgap and position of HOMO (valence band edge) and LUMO (conduction band edge) is very important in device structure, there needs to be a smooth gradient between these values through the device (i.e., type II junction) for charge transport.^[26] There is also a need for blocking movement of electrons and holes through the device so neither can pass the entirety of the device to suppress charge back flow.^[28,29] This is achieved by creating potential wells or energy barriers that the charge carriers cannot pass through. These wells and passages can be controlled by changing the material in the layer and by changing the thickness of the layer to affect charge mobility.^[30]

A basic PC structure includes just two layers, the electrodes which can sit on the same surface of the device, and the PA layer and is the simplest of the structures.^[26] This is because it simply takes the photocurrent from the PA layer and outputs it at the electrodes. As such it is not a highly controllable device and is not as efficient as the current flow is not controlled, it does, however, have a very fast response time so is good for high-frequency imaging due to the electron-hole pair generation simultaneously occurring close to each electrode from incident photons as there are no other layers for transport.^[31,32] It is also typically the thinnest of the device structures and therefore can be used in more different scenarios where space and flexibility are constrained.^[33,34,35]

A basic PT structure includes four layers, the electrode layer, the PA layer, a dielectric layer, and the gate layer.^[26] This leads the device to function as a transistor, where the photocurrent generated in the device can be controlled by the bias across the source and gate. This leads to many different functions, typically in an image-sensing context where the bias on the device can be controlled directly through the device to allow for higher photoconductivity gain by delocalizing trap states.^[26]

The PDD structure is the most universal device structure used in optoelectronics as it is very tuneable by exchanging layer materials and thicknesses.^[26] However, it is a bulky and difficult to work with structure when it comes to image sensors or detectors as it is more complicated to fabricate and is typically too slow at receiving signals to be used easily for real-time imaging due to the increased thickness, charges must move further to affect the current so there is a delay between input and measurement, this is where PC and PT devices are generally more convenient.^[31,32,36,37]

PC devices are the most simplistic of the device structures, and are used extensively in astronomical measurements, particularly with cosmic microwave background observations.^[38] The single optically active layer makes fabrication for large-area devices easy and as such it is a suitable structure for these sorts of measurements where the measuring device is large in scale. It typically would require a form of focusing of a light source onto the surface to detect the relevant wavelengths in a small sky area for usage in telescopes.^[38] When used in this context, it is almost always in tandem with a color filter.

The PT structure is arguably the most useful device structure as it allows for a control of the flow rate of current through the device. The addition of a gate to control current flow through the device allows for more accurate usage in PDs and allows for easier distinguishability between pixels, increasing resolution. The response time of a PT device is also far superior to that of the PDD device, meaning it can be used for live displays more easily, however, the response time is still shorter than that of the PC device.^[34,36,37] By decreasing the size of these devices, one can also increase the resolution of either image sensors or displays.^[35]

1.2. Image Sensors

Image sensors are the next logical step on for PD devices including color recognition, and image sensing (steady and dynamic). Image sensors are already used frequently in many aspects of everyday life and, following the trends, will continue to be used for progressively more applications.

The basic idea of an image sensor is a simple array of PD devices set up to measure different wavelengths of light, and therefore be able to create an image from the intensities of each individual wavelength. For example, for a typical visible light image sensor there might be three PDs set up as a single pixel for red, green, and blue detection (RGB), to allow for easy conversion to a display. There are various ways to arrange these pixels that have been explored and some other methods for detection of these wavelengths of light.^[2,39,40,41]

Historically, the most common form of image sensor was a silicon-based PT device that would have RGB or IR filters attached to different pixels to allow for image sensing.^[42,43,44] This Charge-Coupled Device (CCD) display was originally designed in the 1970s and allowed for digital imaging. More recently Complementary Metal Oxide Semiconductor (CMOS) sensors have been used, as they are far more energy efficient, faster, and can have a higher resolution.^[45,46,47] The latest developments in this area, however, are for QD and organic-based image sensors.

The main limitations of silicon-based CCD detectors, is their thickness and the unwanted IR absorption for use in RGB. CCD detectors are required to be thick due to the absorption length at the required photon energies for absorption, sometimes more than 100 μm .^[48] Silicon has a very small indirect bandgap, 1.1 eV at 300K, which allows for NIR and shorter wavelengths to be absorbed by devices, as such, a filter must be used for silicon-based image sensors in order to realize RGB color recognition.^[42,49] These filters often need expensive materials such as various different forms of non-emissive plastics to be fabricated, and they are bulky which defeats the purpose of using silicon as it is typically a cheaper more common material to use for these detectors.^[42,44,50] The thickness of the devices is also an issue as it means that devices need to be bulkier in general to function, this can be a problem for some larger device structures, as saving on space is generally a good idea, both functionally and financially. The thickness, combined with the brittle nature of silicon, also constrains the use of these types of detectors in flexible devices, although methods have been developed to get around this issue by using different device structures such as imbedding detectors in a flexible film.^[51,52,53]

CMOS devices suffer from similar issues to silicon CCD devices, they are cheaper but still costly and have too large an absorption window and are brittle.^[45,46,47] This makes it tough to make these devices thick enough to absorb efficiently without losing flexibility. They also require filters of some kind to create any color sorting effects, however, the range of materials for CMOS allows for an easier option to create color-specific pixels. CMOS sensors function by using a series of p and n type transistors in tandem, allowing the charge buildup generated from the absorption of light to be used as a signal in a detector which can be released by switching the circuit between the p type and the n type transistors.^[45,46,47]

One of the major issues with image sensors is how to create smaller pixels and higher-density patterned devices. In order to achieve pixelation and patterning many different approaches can be used. The most common of these approaches is to pattern the electrodes on larger area thin film devices. This can be done through masked evaporation,^[54] masked sputtering,^[55] inkjet printing,^[56] etching,^[57] photolithography,^[58] electron beam photolithography,^[59] or direct laser writing^[60] to name just a few, however, these methods can be time-consuming, and expensive. One method of deposition for photodiode devices that avoids these issues, is to electrochemically deposit the layers. The process by which this works is electrodeposition, through electrophoresis, which facilitates mass transport of particles to a surface to allow for deposition onto that surface. This can be used to create intricate designs of devices by using various different electric fields and electrical properties to change the deposition.^[61,62]

1.3. Carbon Footprint

A brief explanation of carbon footprint is required to understand exactly what the impact these methods have on the environment is. The carbon footprint of something is defined as the total amount of greenhouse gases that are emitted into the atmosphere during a process and is typically measured in tonnes of CO₂ equivalent.^[7,63,6] The larger the value for a process the more damaging this is for the environment, although in some cases it is not obvious that it could be damaging, and only through research of the effects of various chemicals in the atmosphere can the damage be determined. An example of this would be the usage of ChloroFluoroCarbons (CFCs) in refrigerators and aerosols during the 1980s,^[64] which it was discovered was having a larger impact on the atmosphere than was originally understood. This is relevant as some of the chemicals used in the processing of semiconductor devices are almost on a similar scale in terms of the damage they can cause per unit volume.

Methods such as plasma sputtering, and thermal evaporation have a large impact on the environment primarily due to the gases used in industry in the processing methods for the devices.^[7] These gases include sulfur hexafluoride, various halide gases, and siloxane, all of which are known to contribute heavily to the greenhouse effect, in many times excess of similar volumes of CO₂.^[7] For sulfur hexafluoride the equivalent CO₂ tonnage is 22800 to 1,^[7] which although the gas is predominantly used as a dopant gas to aid certain evaporation processes, is not ideal to be pumping into the atmosphere as there is no way to cleanly process the gas after use.

The benefits of using a solution processed method as opposed to traditional methods in terms of carbon footprint is fairly simple, these gases are not used, there are not as large amounts of energy used to power the devices, and the only source of waste comes from the materials used and the solvent that carries the particles. As such the carbon footprint of fully solution processed photodetectors is limited almost solely to the fabrication of the materials used which can be limited in the cases of most organic polymers and quantum dots.^[65,66]

One issue with solution processing methods is the lack of patterning in many methods, which can lead to the use of

Table 1. Showing a rough comparison between different methods of fabrication and their quality and carbon footprint.

Method	Layer conformity	Pattern ability	Carbon Footprint	References
Spin Coating	High clarity of layer deposition, relatively low surface roughness	No inherent patterning possible	Low	[3, 67]
Dip Coating	Low clarity of layer deposition, high surface roughness	No inherent patterning possible	Low	[13]
Inkjet Printing	Relatively high clarity of layer deposition, low surface roughness	Patterning is easy to achieve to micron level	Very low	[14, 68]
EPD	Relatively high clarity of layer deposition, low surface roughness	Patterning is easy to achieve to micron level	Very low	[18, 69]
Thermal Evaporation	Extremely high clarity of layer deposition, very low surface roughness	Patterning is possible and is aided with external patterning methods	High	[7, 70, 71]
Sputter	High clarity of layer deposition, low surface roughness	Patterning is possible and is aided with external patterning methods	Very High	[7, 72, 73]

photolithography and direct laser writing to pattern the devices, which again add to the carbon footprint of the process which is not ideal (Table 1).

1.4. Organic Based Photodetectors (OPDs)

Organic-based photodetectors are a good basis for these devices. Due to their broadband absorption, semiconducting organics can be used in PD devices to great effect. Typically, these detectors have to use filters to achieve color purity, however, and even then, true color fidelity is hard to achieve. There are various means to avoid using color filters for OPDs which shall be covered later in this review.^[74,75,76]

The main premise behind the device remains the same, however, the PA layer is replaced by a semiconducting organic molecule or polymer, examples of which are shown in Figure 2. This organic will then absorb the incident photons and convert them into electron-hole pairs and the process is the same, however, the organics have a tuneable wavelength range. By changing the moieties of the organic, one can change the range in which the device will absorb, which gives it a large advantage over silicon-based CCD devices.^[8,9] As well as this, the polymers have their own unique absorption spectra, which is less of an on-off switch for absorption. This means that they have a range in which they absorb very well, and outside of that range, at higher energy, they absorb less well due to how the interactions occur, the higher the energy of the photon, the lower the chance of interaction with the organic. In the range that the organic will absorb, the organic will absorb at ≈ 3 orders of magnitude larger than that of silicon for the same range.^[48]

However, these benefits come with weaknesses. These organics tend to be unstable under larger charge flows and have a tendency to decompose under many different conditions including being in an oxidizing atmosphere, high light intensity or heat exposure.^[12,77] Once these organics have decomposed, even slightly, their absorption spectra will be completely different, the charge transport properties will change, and the devices involving them will cease to function as they had previously, typically ceasing to function at all. Due to the molecular nature of the organics, they tend to have a less regular overarching structure, as such, they tend to be harder to organize into a regular and periodic film, they will always be amorphous. This leads to a decrease

in device performance inherently and gives fabrication a more random nature. As a result of this, a lot of research is done into how to produce more uniform films using organics.^[33,78]

1.5. Colloidal Quantum Dot Based Photodetectors (QPDs)

Using Colloidal Quantum Dots in photodetectors for use as image sensors inherently makes a lot of sense due to the characteristic properties that QDs have. The main properties of interest include the tuneable bandgap, the sharp excitonic peak, and the high photoluminescence and quantum yield which allow for good color fidelity and increased efficiency.^[10,11]

QDs are a type of nanocrystal that is encapsulated by a ligand to stabilize the nanostructure as shown in Figure 3. This stabilization aids in preventing the crystals from agglomerating and also affects the QD's properties. Changing the ligand that is encapsulating the QD will typically also affect the polarity of the QD in solution, the zeta potential, the pH, and the bandgap of the QD.^[4,79,80] Ligands are usually changed from non-polar to polar for use in different structures to avoid erosion from similar solvents or from short chain to long chain to either improve the charge transport in the layer or to decrease the interaction between QDs respectively.^[79] These ligands can be any sort of molecule that will interact with the QD and remain "stuck" to the surface, typically being an organic or a halogenated molecule.^[79]

QDs are unique when being used in this context due to their characteristic absorption and by extension emission. QDs are most simply considered a hybrid between a bulk semiconductor and a single atom, they have characteristics of both. This is due to the size of the QD particles, typically between 2 and 10 nm.^[10,11] The particles being in this size range allows for a phenomenon known as quantum confinement to occur when interactions with this particle take place, due to their size being comparable to their Bohr exciton radius.^[10] This phenomenon gives rise to both atomic and bulk behavior, the HOMO and LUMO levels of the QD split to be atomic and discrete in nature at the boundary, but as you extend into the band structure the energy levels become continuous and more akin to that of a bulk semiconductor.^[11] With these characteristics, the absorption profile of a QD has a series of discrete peaks based on the atomic nature of the crystal, and a broader peak due to the bulk nature of the crystal, giving a unique spectra.^[10,11]

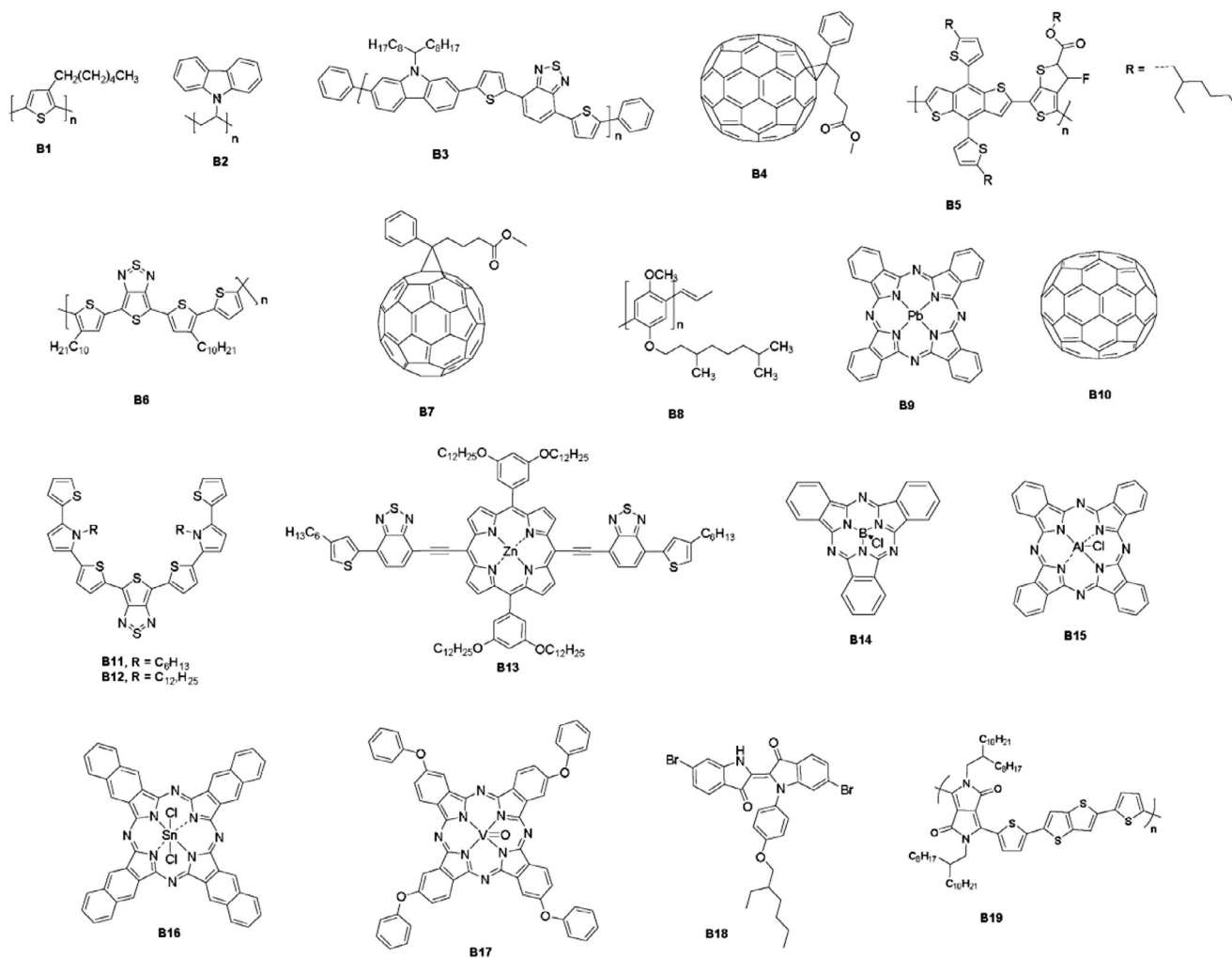


Figure 2. Examples of various organic molecules and polymers used in PDs, B1-19, typically used for broadband (B) PDs from Jansen et al. Reproduced with permission.^[2] 2015, John Wiley and Sons.

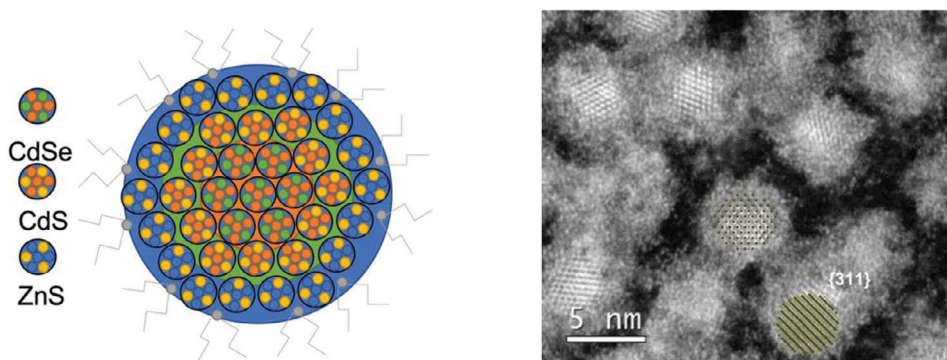


Figure 3. Colloidal Cadmium Selenide/Cadmium Sulphide/Zinc Sulphide QD visualization from Osypiw et al. Reproduced with permission.^[11] 2022, Royal Society of Chemistry. and a TEM image of PbS QDs from Hou et al. Reproduced with permission.^[147] 2023, American Chemical Society.

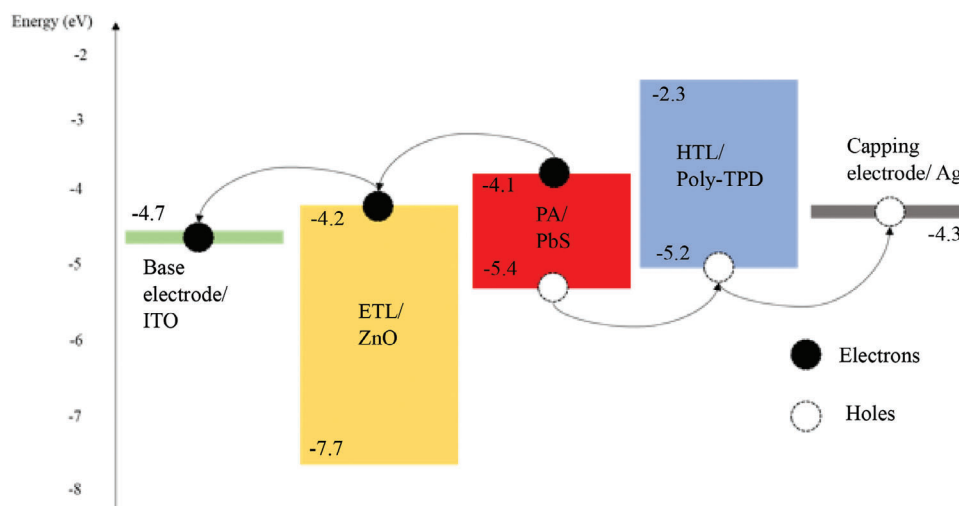


Figure 4. Demonstration of bandgap structure for a typical PDD device with ETL and HTL. Electrons-hole pairs are generated in the PA layer, where they then step toward the relevant electrodes as shown. The values used are for an ITO/ZnO/QD/Poly-TPD/Ag, from left to right, structure.

When fabricating QPDs the basic structure is the same as for a general PD, however, the thickness of the layers needs to be adjusted. This is due to the high extinction coefficient in QDs.^[81,82] Electrons, holes, and photons all have high extinction values in QDs, which means that, generally speaking, QPDs have to be thinner overall than other PD devices. The device structure can also be changed by changing the ligand on certain layers of QD in the device.^[79,80] This is akin to doping a PA layer and can be done to achieve a quantum well to block transport of charges in certain directions by changing the bandgap and HOMO LUMO positions on the energy level diagram as shown in **Figure 4**.^[83]

2. Color Specificity

In order to achieve specific color absorption, a few methods can be used. These typically consist of using a form of color filter array, or by stacking layers of different absorbing materials on top of each other. The color filter array is a form of external color separation, usually performed by an auxiliary structure separate to the device itself. There are also internal methods of color separation by affecting the charge carrier collection in the device. Of these, the filter arrays are more common in commercial use, as they are far easier to produce though they reduce device performance.^[2]

2.1. External Color Separation

The filter arrays typically involve a series of pixels being devoted to a certain color, for example the Bayer filter in a 16 pixel array, 4 would be red, 8 would be green and 4 would be blue, as shown in **figure 5A**.^[39] This mimics the way in which the human eye functions as it is inherently more sensitive to green. However, the main issue with this method is the overall pixel size is large, and analyzing the signals can become difficult during the demosaicing process which can lead to decreased color constancy. This demosaicing process is a series of signal processing algorithms

that allows for the resolving of the signals from each color, to allow for a full RGB color image.^[84] Another issue with this method is that the filter itself absorbs around two-thirds of the useful incident light, so naturally the efficiency will drop.

Another method used is to have the filters on a rotating table and take separate exposures with each filter as shown in **Figure 5B**.^[2,41] However, as each frame developed would take more than three times as long to process due to the filter changes, this is significant problem as images can shift during the time between each color frame, so this method can only reliably be used for still imaging. As such this is only used for still frame cameras or in certain detectors for research purposes.^[41]

The final common method is to use a beam splitter to allow for high-quality imaging as shown in **figure 5C**. This allows for the incident light to be separated into its component parts to filter for certain wavelengths by passing the light through a prism. The refractive index and angles in the prism allow for the separation of RGB wavelengths to be picked up by a PD dedicated to that color. These typically make the highest quality images, though there is limited room for miniaturization.^[2,41]

There are many other methods that are less commonly used, such as integrated color pixels, micro color splitters, and the use of external nanostructures to optimize certain wavelengths.^[2] There is continued research in this area though it is not the focus of this review.

2.2. Internal Color Separation

Another way of achieving a filter on an image sensor is by changing the PA layer or device structure to focus on particular wavelengths, considered a material-based approach to light filtering. One method of doing this for RGB sensors is to stack a layer of blue absorbing material on top of green absorbing material on top of red absorbing material for a single pixel creating a stack of RGB from bottom to top. If the thicknesses of the materials are optimized to match the penetration depths of the relevant

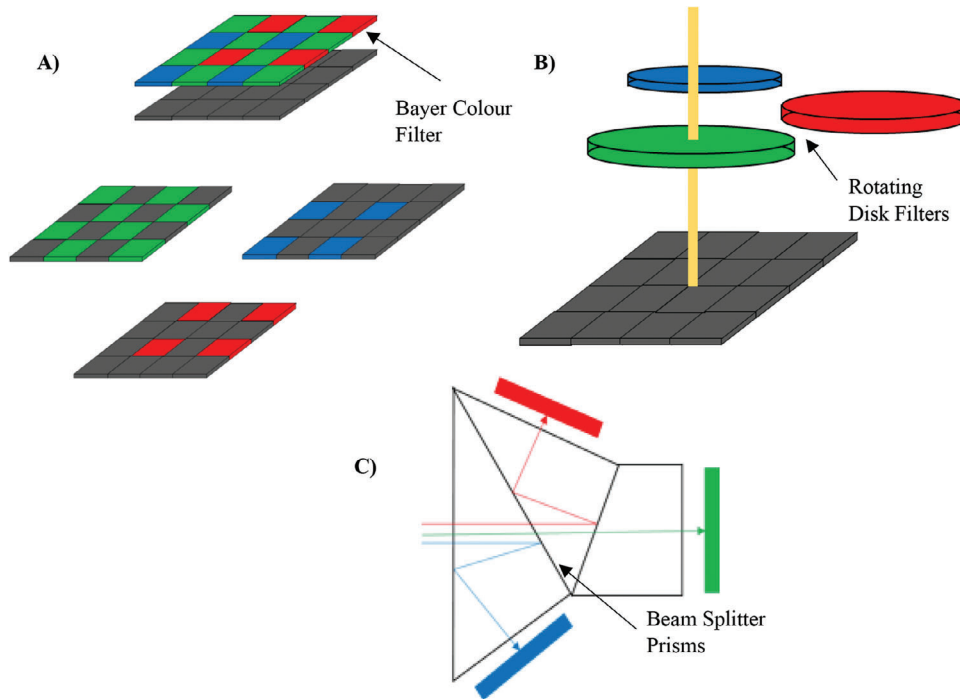


Figure 5. External filter types, A) Bayer filter array is placed over a pixelated photodetector to illuminate specific pixels with specific wavelengths with the component parts of the filter displayed underneath, light is incident from the top, B) rotating disk rotates the filters in and out of the incident beam (yellow) to illuminate the photodetectors en masse, and C) beam splitter prisms split off selected wavelengths to select wavelengths using total internal reflection and refractive index.

colored photons, then with signal processing the contribution of each color can be calculated and a color-detecting device has been made.^[85,86] This effect of the different absorption profiles of different wavelengths through the device is the most prominent method of creating filter-less image sensors. The effect of using this structure in a device has many benefits, there is much higher fill factor for the pixels and increased efficiency as more light is absorbed per pixel. However, there are also downsides to this structure, as the crosstalk between pixels is hard to eliminate and provides poor color purity.^[2]

Another method is Transverse Field Detectors (TFD). These use the charge carrier mobility of the devices to control the color selectivity of the device, typically used in CMOS devices.^[87,88] An electric field is placed across the device to generate charge carriers at different depths in the device, therefore allowing certain wavelengths to be emphasized in the specificity of the device by increasing the efficiency at those wavelengths.^[87,88] This is a particularly useful method as it implies that different wavelengths can be specified at different biases across the device, as such it is one of the more interesting areas for the future.

A final method would a similar method to TFDs in terms of color selection and the overall usage of generating charge carriers in a certain manner but without the electric field, simply using the thickness of the junctions to achieve the same effect. This is known as Charge Collection Narrowing (CCN) and will be discussed in more detail in Section 5.2.1.^[30,74] This can also be combined with TFDs to create an effect called Charge Injection Narrowing (CIN) which will again be discussed in more detail later in Section 5.2.3.^[76,89] Changing the material of the PA layer

will also affect the performance of the device, sometimes creating a filtered effect.

3. Figures of Merit

Efficiency and performance of PD devices are measured in different ways, the photo responsivity, the quantum efficiency, the detectivity, the noise equivalent power, and the linear dynamic range, some state of the art values are shown in (Table 2).^[2,26] There are other means of comparing performance, however, these are the main methods. Within these parameters are other important parameters of note such as the absorption spectra and the dark and noise currents.^[2,26]

3.1. Responsivity and Quantum Efficiency

The photoresponsivity (R) is a measure of the ratio of input power to output current. It is a very basic way of characterizing PD devices by essentially comparing how much current is output by the device given the irradiance of the light on the device.^[2,26,92] A more fundamental way of describing this sort of device performance is through the External Quantum Efficiency (EQE), which is measure of how well a device can convert photons into electrons or holes and then transport them to the electrodes.^[2,26] This is a better way of comparing devices as it shows a more fundamental reaction occurring in the device, the excitation of electrons from the valence band to the conduction band after absorption of an incident photon.

Table 2. Figures of merit for state-of-the-art devices using different detection methods.

	Detectivity [j]	EQE [%]	Wavelength [nm]	FWHM [nm]	Response Time [ns]	Pixel Size [μm]	Reference
OPD-CCN	$\approx 10^{12}$	7	950 and 680	<90	–	–	[30]
OPD-ILD	$\approx 10^{13}$	49	760	60	–	–	[75]
OPD-CIN	9.73×10^{13}	2.51×10^5	650	40	67×10^6	–	[89]
QPD	4.4×10^{11}	25	1240	–	70	–	[90]
OIS	$\approx 10^{12}$	–	532	–	–	250x300	[15]
QIS	2.1×10^{12}	16.5	400-1300	–	300×10^6	15x15	[91]

The responsivity can be calculated as shown in Equation (1),^[2,26]

$$R = \frac{I_L - I_D}{P_{in} S} \quad (1)$$

where I_L is the photocurrent, I_D is the dark current, P_{in} is the power of the incident light as measured on the surface and S is a measure of the surface area that the light is incident on. From the equation, it is clear that it is simply a comparison of the current generated in the device to the power of the light incident on a defined area.

The EQE can be calculated through the use of Equation (2),^[2,26]

$$EQE = \frac{R h \nu}{q} \quad (2)$$

where $h \nu$ is the energy of the incident photon and q is the coulomb charge. As can be seen, this is a scaling of the responsivity with respect to the photon energy and the elementary charge

and is more intrinsically linked to the phenomena occurring in the device.

When applying this aspect of photodetectors to image sensors, the ideal values of these quantities would change. When used in broadband photodetectors, the responsivity and EQE should be as high as possible in all regions, as the aim of the device is simply to detect incident photons as shown in **Figure 6**. However, when making an image sensor, the aims are different, specific wavelengths are to be targeted for detection, meaning that the responsivity should still be high, but the EQE should only be high strictly for the wavelengths that are intended for detection.^[2,74] As such, the device should also be designed in such a way as to avoid unwanted absorption by choosing materials that only absorb in certain ranges.

Another way to get around this particular issue is to change the thickness of the different layers in the device to affect charge transport and affect the EQE by allowing some charges to reach the relevant electrodes, whilst preventing others from doing so.^[74,75] This allows for the absorption of some layers to be suppressed as the relevant charges extinguish before they can reach

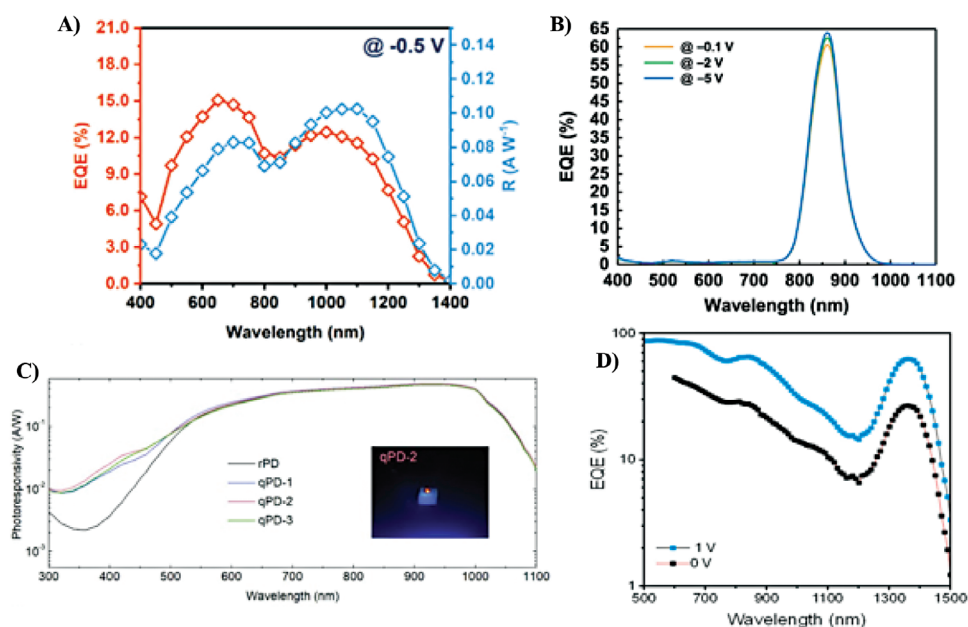


Figure 6. A) EQE and photoresponsivity comparison for an OPD device from Zhang et al. Reproduced with permission.^[148] 2024, American Chemical Society. B) EQE spectra from a narrowband OPD device from Xie et al. Reproduced with permission.^[149] 2020, Springer Nature. C) Photoresponsivity of InP based QPD device by Huang et al. Reproduced with permission.^[150] 2023, Elsevier. and D) EQE spectra of a QPD device by Atan et al. Reproduced with permission.^[151] 2023, American Chemical Society.

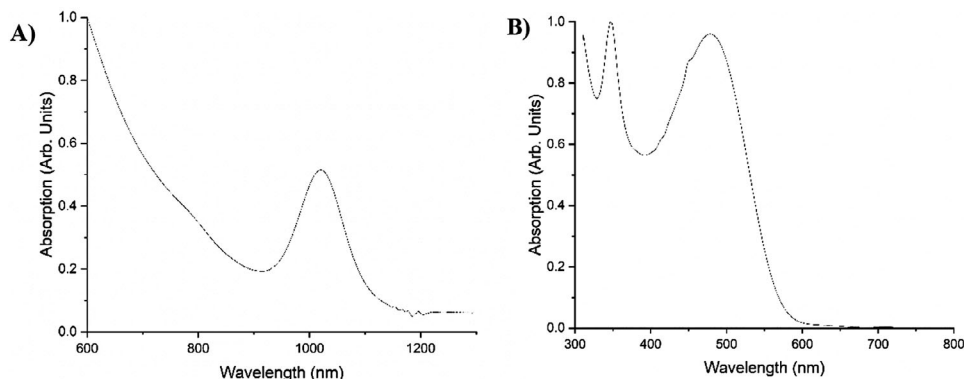


Figure 7. Example absorption spectra of, A) PbS QDs with oleic acid ligands and B) P3HT:PCBM 15:12 organic blend.

the electrodes. Due to this, the EQE is heavily dependent on the charge transport in the device due to the wavelength specificity and will be discussed more in Section 5.2.

3.2. Absorption Spectra

In the previous section, the absorption of the materials used in the devices was mentioned. For organics and QDs, the absorption spectra are usually very different. QDs have a characteristic absorption peak that arises from the quantum confinement effect that makes them quantum dots as shown in Figure 7A. There are multiple peaks from this confinement effect similar to atomic absorption, combined with the bulk absorption of a generic bulk semiconductor.^[11,93] Organics tend to be more varied in their spectra and can range from very broadband to quite narrowband. As such, the materials used in OPD or QPD devices can give a wide range of different types of absorption spectra, one of which is shown in Figure 7B.^[2,94]

To quantify this typically the values of the FWHM, the absorption onset, and absorption cutoff are used.^[94,95] This allows description of the peaks, and the shape of the absorption particularly for organics, which can have uneven spectra with multiple

broad or narrow peaks. The bandgap of the material is also obtained through the absorption spectra, the absorption onset is related to the bandgap which is used in planning the structure of devices and can be obtained by creating a Tauc plot.^[96]

3.3. Dark Current and Noise Current

The dark current of a device is the current that inherently runs through the device when there is no external excitation, caused by the differences in charge carrier mobility, the doping and trap density, and the work function of the electrodes. The residual heat of the device allows for the excitation of charges, causing current to flow. Dependant on the characteristics of the material, the doping type, and density, this can be large or small as shown in Figure 8.^[2,26,97]

Dark current is generally quite inconsistent due to the means by which it is produced so it can be challenging to remove from the signal output from the device. However, the dark current can also be removed from the device by introducing non-conductive blocking layers into the structure to suppress this background charge flow.^[27] The noise current is the total overall background current in the device. This is a combination of different sources of “noise” in the current such as the shot noise^[98] and differences

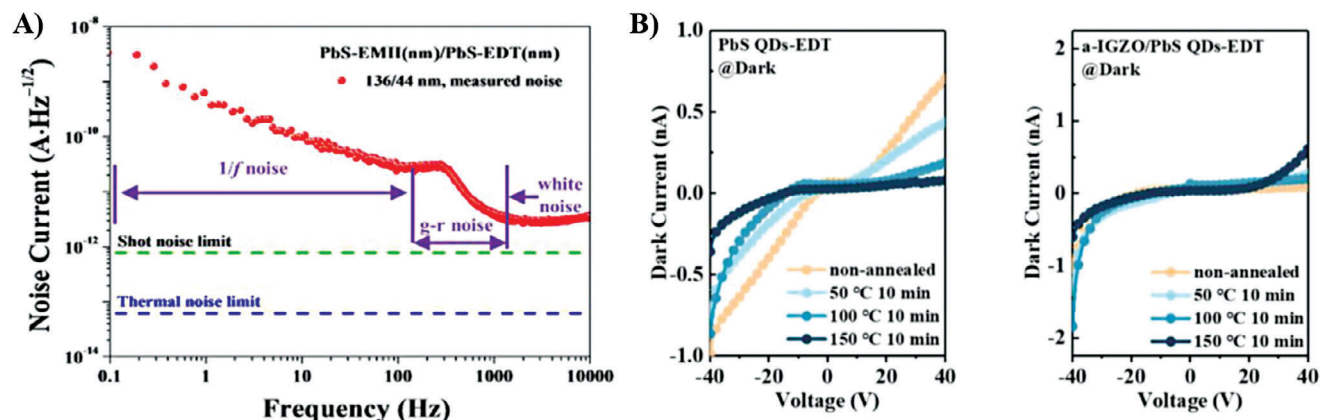


Figure 8. A) Demonstration of noise current and different regimes of importance from Equation (3) from Gong et al. Reproduced with permission.^[152] 2022, American Chemical Society, and B) The effect of different conditions and added layers on the dark current showing the correlation between higher order in thin films and a decrease in dark current at different voltages from Zhang et al. Reproduced with permission.^[153] 2023, American Chemical Society.

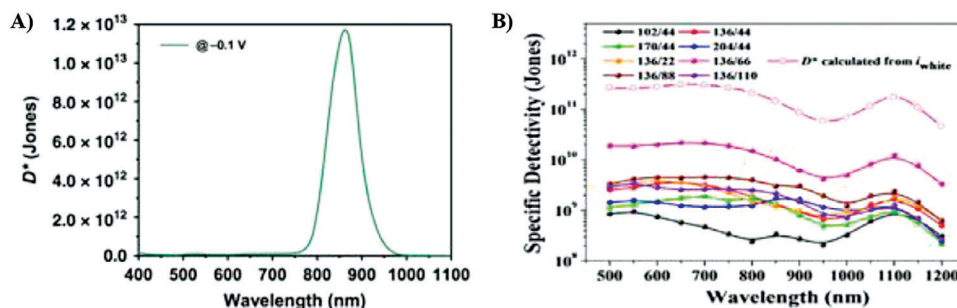


Figure 9. A) Representation of narrowband OPD detectivity from Xie et al. Reproduced with permission.^[149] 2020, Springer Nature. and B) detectivity of broadband QPD from Gong et al. Reproduced with permission.^[152] 2022, American Chemical Society.

in thermal energy through the device.^[2,99] This can be written in the form,^[2]

$$i_{\text{noise}} = \left(i_{\text{shot}}^2 + i_{\text{thermal}}^2 + i_{1/f}^2 + i_{g-r}^2 \right)^{1/2} \quad (3)$$

There are also some complex components of the noise current such as the 1/f noise and the generation-recombination (g-r) noise.^[100] These values typically would be ignored in a more conventionally structured device with high homogeneity in each layer, however, in more randomly ordered layers, such as in OPDs or QPDs the 1/f noise and g-r noise can reach levels where they impact on the calculation significantly.^[101] Due to the frequency-dependent nature of the 1/f and g-r noise, at lower frequencies the contribution from these parts is larger than expected and so the noise current will be significantly larger than expected. This is important as it will affect another important characteristic of the devices, specific detectivity.

3.4. Specific Detectivity (D) and Noise Equivalent Power (NEP)

The specific detectivity, D , is a measure of the sensitivity of a device to incident light. It is essentially a measure of the lowest intensity of light that can be measured by the device shown in **Figure 9**. This can be expressed in the form,^[2,101,102]

$$D = \frac{R}{\sqrt{2q}i_{\text{noise}}} \quad (4)$$

where all values have their previous meanings. In the case of a more conventional, well-ordered device, not an OPD or QPD, i_{noise} can be replaced with I_D , as the noise current would be almost negligible as mentioned in Section 3.3. Specific detectivity is measured in units of $\text{cm Hz}^{1/2} \text{W}^{-1}$. This is to say that it is the signal to noise ratio of a 1 cm^2 area of the PD with a 1 W incident power detected at 1 Hz bandwidth.^[2,103] This means that it is heavily related to the Noise Equivalent Power (NEP).

The NEP, is similar to the detectivity in that it is a measure of the ability to distinguish between noise and photocurrent from the input power and can be written as,^[2,102]

$$\text{NEP} = \frac{S\Delta f^{1/2}}{D} \quad (5)$$

where all values have their previous meaning and Δf is a measure of the electrical bandwidth. It is important to note that the specific detectivity and the NEP are reciprocal to each other, as such they represent very similar characteristics of the PDs. Typically, the detectivity is more commonly used and represented in reported research, though often there are oversights in the calculation for the noise current. Due to this, measured noise current has been used more frequently in recent publications allowing for more accurate detectivity values that do not overestimate.^[30,74]

As detectivity is so important in PDs, it is equally important to understand how to improve it. There are two main methods to do this, either by lowering the noise current, or by increasing the responsivity or EQE. In OPDs the EQE is typically limited to 100% without an external bias, however, in QPDs the EQE is not limited to the same value due to multiple exciton generation.^[93,104] As such the process for optimization of the two different types of PD is very different and shall be explored later in this review.

3.5. Linear Dynamic Range (LDR)

A dynamic range describes the operational range of a PD, the range of light intensity over which a detector can distinguish between signal and noise. This is typically defined by a ratio of the maximum current and the minimum current that can be measured in the device, where the minimum current would be the noise current or dark current of the respective devices. In the case of OPDs and QPDs, a Linear Dynamic Range (LDR) is the most logical type to use as it is a derivative where responsivity is constant, and it specifies an order of magnitude that the response is linear over.^[105,106]

At low light intensity the photocurrent is linear with respect to light intensity, however, as the light intensity increases past the I_{Max} , the linearity is lost and the responsivity decreases. The point at which this occurs depends on the charge mobility of the materials used and the recombination rate coefficient.^[107,108] The lower limit should theoretically be i_{noise} , however, if a bias is placed across the PD sometimes the linearity can be lost at lower light intensities. As such, it is better to measure the LDR experimentally, rather than calculate using the theoretical values.

To express the LDR, using the normalized dB unit range is the most convenient, so the LDR can be shown as,^[2,26]

$$\text{LDR} = 20 \log \left(\frac{I_{\text{Max}}}{I_{\text{Min}}} \right) \quad (6)$$

There are various ways to increase the LDR, increasing the maximum threshold for the linearity, or decreasing the noise current. Increasing the maximum threshold can be accomplished by increasing the slower charge carrier mobility, decreasing the series resistance, decreasing the junction thickness, or by increasing the photocurrent.^[107,108]

4. Solution Processed PDs

The topic of this review is the fabrication of these PD devices through solution-processed means. There are many different methods for deposition of solutions for the purpose of PD fabrication as mentioned previously. Different methods include spin coating, inkjet printing, dip coating, and EPD. Each of these methods has its own benefits and drawbacks depending on the exact device that is being manufactured.

4.1. Spin Coating

Spin coating is an established method in which the solution is deposited onto the substrate, and the substrate is spun at high rotational speeds, usually more than 600 rpm, to apply centrifugal force onto the solution to spread it thinly and evenly on the surface.^[109] The solution is spread evenly across the substrate due to the centrifugal force and substrate solution-surface interaction which then allows for evaporation to occur on the thin film of solution to leave behind the solute. This will lead to a thin layer of solute particles left behind on the surface in a thin film that can be used in devices. The spin speed can be changed to affect the thickness and roughness of the films and is very dependent on the particular solvent and solute mixture used to coat. It is possible to spin multiple layers on top of each other and this is how the majority of devices are produced for general research in device structure and performance.^[11]

Whilst spin coating is a very quick and easy method for thin film deposition, there is limited ability to pixelate devices with this method except using pixelation on the electrodes which can lead to poor signal resolution in image sensors.

4.2. Inkjet Printing

By contrast inkjet printing takes approximately the same length of time to make a small area device as a large area device and can also include pixelation in individual layers and allows for all layers to be made in the same way, it does not require thermal evaporation, sputtering or etching to deposit electrodes.^[110,111]

The inkjet printer works by the use of a piezoelectric and vacuum gas system.^[110] The most common drop on demand printers use a piezoelectric system to pump the ink fluid through small diameter nozzles to control the size and shape of each individual drop as shown in Figure 11A. This is done by applying a voltage to a piezo material changing the shape and applying a force to the ink increasing the pressure at different points along the nozzle canal to form the droplet.^[110,111]

With increasing work with nanoparticles and in particular using nanoparticles in electronic devices in the past 30 years, the

ability to deposit these onto surfaces has become increasingly important. Nanoparticles can easily be deposited through the inkjet printing process as well as through other processes.^[14,111] However, the reason for inkjet printing being picked up more recently as a means of fabricating devices is due to its ability to change the film design easily and quickly due to the ability to program exactly where each droplet will fall to increasing accuracy. In a similar fashion to 3D printing, inkjet printing has potential to be the future of semiconductor device fabrication.

The most important aspect to consider when inkjet printing is the ink formulation as this is the main method by which the drop size and shape can be controlled. The viscosity and surface tension of the ink are required to be within a certain range dictated by the inverse Ohnesorge number, given in equation 7,^[112]

$$\frac{1}{Oh} = \frac{Re}{\sqrt{We}} = \frac{\sqrt{\gamma \rho a}}{\eta} \quad (7)$$

where γ , ρ , a , and η are the surface tension, density, nozzle diameter, and viscosity respectively. This allows for the formation of single droplets of a good shape and size; however, the boiling point of the ink has to be taken into account for the drying process of the drop as well. This gives rise to the coffee ring effect shown in Figure 10C.

The coffee ring effect is one of the main difficulties in inkjet printing. Due to the capillary flow along the substrate, the surface tension and surface interaction between the ink and the substrate drags the ink, and by extension the particles suspended in it, along the surface. This creates an imbalance in the particles distribution in the ink which can lead to an uneven printed film. This is controlled by changing the solvent of the ink to affect the surface tension, the zeta potential of the ink, and the boiling point to create a more even film.^[14] As such, different qualities are required for a good printing ink as opposed to a good spinning ink.

4.3. Dip Coating

Dip coating is an established method in other areas of material fabrication, generally used for paints or protective layer coating on metals.^[11,13] However, it is being applied to other areas of material science. To make devices each layer can simply be dipped into with the substrate and the solution mix will cling to the substrate in a thin layer and evaporate leaving behind the desired solute. However, this is a relatively new research area, as such it is unreliable at the present moment. The basic premise is that by changing the speed at which the device is drawn through the interface of the fluid, the thickness of the layer that clings to the device and ultimately dries on it is also changed. This is typically affected by the viscosity of the fluid, the surface tension of the fluid, and the boiling point of the fluid all of which impact the shape of the meniscus formed at the interface and the drying rate of the film, although there are different models that incorporate other features.^[11] As such, dip coating is a very simple process, but has a large region of error in how it can be done effectively.

Dip coating suffers from similar limitations to spin coating in that there is limited ability to pixelate devices. It also requires larger volumes of solution for dipping as you generally require more solution to fully coat a device of the same size, or

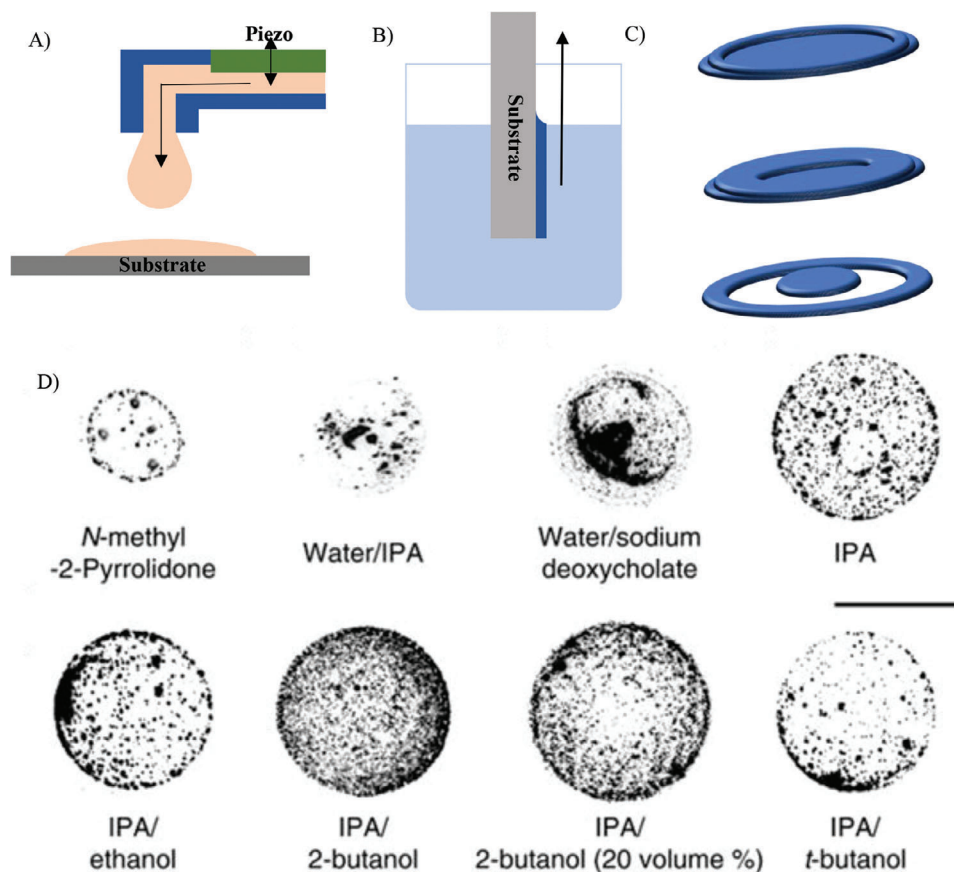


Figure 10. Inkjet printing and dip coating processes. A) The piezo (green) oscillates creating a pressure wave in the ink by the nozzle, causing a droplet to form and drop from the nozzle. B) A substrate is dipped into a container with ink and drawn out at a speed dictated by the thickness required. C) Different forms of coffee ring effect that can occur if an unfavorable ink is printed. D) Various different coffee ring drying patterns from Hu et al. Reproduced with permission.^[68] 2020, AAAS.

interactions with the container also have to be considered in the dipping process. However, the main trade-off for this is that much thicker layers can be deposited by dip coating than by any of the other methods mentioned above.^[11,13] Dependent on the type of device that is being fabricated, dip coating can be more beneficial than other methods, for example in the case of a depositing a thick PA layer to increase the total absorption, for example in the cases of CCN or CIN.

4.4. Electrophoretic Deposition (EPD) and Patterning

A promising method for producing PD devices is through electrochemistry. This can be achieved by various different means, the main method being through EPD or electrochemical patterning of the devices.^[61,62,113,114]

EPD is achieved by pumping a direct current through a solution with two or more electrodes connected to the circuit as visualized in **Figure 11**. Provided that there is an electrical pathway through this solution, typically from charge carriers inserted into the solution in the form of an ionic salt, this current will pass through from one electrode to another.^[113,114] This current and potential difference allows for the ions and charges within the

solution to move to the relevant electrodes, negative charges to the cathode, and positive charges to the anode. In systems with more than one electrode this can be changed to achieve different forms of charge transport between the electrodes.^[113] When the charged ions contact with the electrodes, there is a chance that they will stick to the electrode at points referred to as nucleation sites and start to form a thin film. These nucleation sites are points at which the potential between the ions and the electrodes is equal and opposite so that the ions are more likely to stay attached after the impact.^[113,114]

4.4.1. Mass Transport in EPD

It is important to note that EPD is a very delicate method that is inherently quite difficult to control completely. There are a lot of different variables which need to be controlled or considered at all times such as the voltage and current, the concentration of the solution, the surface potential of the electrodes, the temperature and pH of the solution, and the proportion of excess charge carriers or electrolytes in solution to name but a few.^[113,114,115,116] The main methods of mass transport in EPD are diffusion, convection, and migration.^[114]

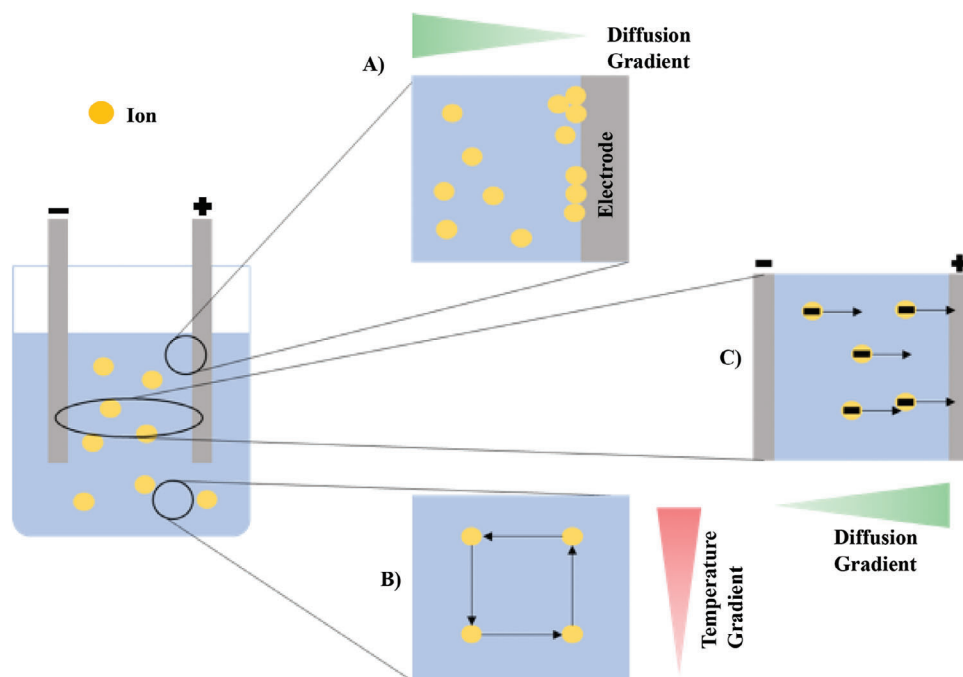


Figure 11. Example setup of EPD showing a two electrode system in solution with electrolyte, the most basic setup, with charges indicated by yellow dots in blue solution and grey electrodes. Affected motion of A) diffusion, B) convection, and C) migration. Gradients of temperature (B) and concentration (A,C) are shown in red and green respectively, darker color indicates a higher value on the curve. For diffusion the concentration is higher to the left, for convection the temperature is higher at the top, and for migration the concentration is higher toward the right.

Diffusion: Diffusion is the attempt of the system to try to become more homogeneous, to try to eliminate any inconsistencies. This is the most basic method of mass transport for an electrochemical system and is solely controlled by the concentration of the solution in the volume. The best way to describe the system is using equation 8,^[114]

$$j = -D_B \frac{d[B]}{dx} \quad (8)$$

where j is the diffusion flux, $[B]$ is the concentration, and D_B is a constant of proportionality. This equation will hold in any coordinate system used.

Diffusion is the main process by which the system will transport charges and is also applicable in the other cases due to the movement of particles. The diffusion gradient of the system also controls the rate at which deposition occurs and affects how the deposited film is structured.^[113,114] Different rates of deposition allow for different growth mechanisms as will be discussed in Section 4.4.2, so controlling the diffusion gradient to influence this is the main method for influencing the finished film.

It is important to note that the diffusion gradient is constantly changing in the system, not just due to the methods mentioned but also due to the deposition itself. As the material is deposited, it is depleted from the solution and is adsorbed to the surface of the electrode or substrate.^[113,114] This means that there is a lower concentration of the material in solution at the surface, so the diffusion gradient will shift to a shallower slope, decreasing the rate of deposition. The term for this is the “diffusion layer”, and it

has a maximum thickness that is achievable calculated by Nernst to be ≈ 0.05 cm for electrodes with millimetre dimensions.^[114,117] For longer depositions, this loss of concentration needs to be accounted for, which is typically done by introducing a fluid flow into the system such as a rotating disk or by using microelectrodes as discussed in more detail later in Section Migration and 4.4.3.^[113,114,118,119]

In practice the concentration of the system will stay relatively constant due to the convection in the solution, either natural or forced. As such the diffusion gradient will become constant once the diffusion layer is fully formed and the deposition rate will be kept constant meaning that for longer depositions the rate of film growth is more constant than for shorter depositions, leading to better film formation.^[114,115,120] However, due to this initial change in deposition rate, the base layer of the films will be rougher and less homogeneous impacting on the quality of the layers deposited above.

Convection: Convection is the result of a mechanical force on the solution, either from thermal and density differences or from an external force such as stirring or pumping.^[113,114] The former can arise simply from the system not being isolated, or from the processes that occur during the deposition, the reaction at the electrodes can be endo- or exo-thermic. This natural convection is hard to control and is inherently random, the only practical way of controlling it is to use external convection. Over a time period of longer than 10 seconds, the effects of this natural convection can become significant enough to completely randomize any process that occurs, which is counter to the effects of diffusion.^[114]

The second type of convection is typically called external or forced convection.^[114] This is generally introduced into the

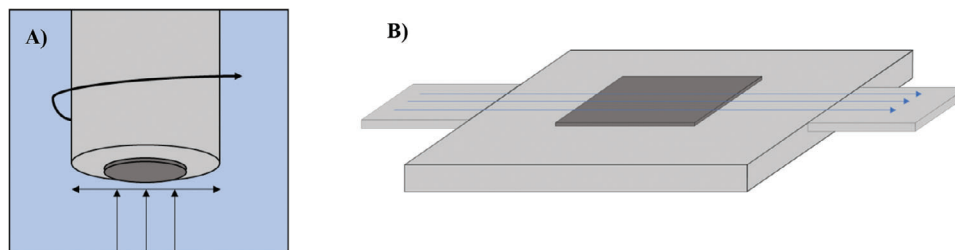


Figure 12. A) Rotating disk electrode and B) flow cell electrode. Arrows indicate the direction of fluid flow.

system to swamp the effects of natural convection. The change in concentration of the solution will be as shown in equation 9,^[114]

$$\frac{d[B]}{dt} = -v_x \frac{d[B]}{dx} \quad (9)$$

where v_x is the velocity of the solution. Again, this can be put into any coordinate system and will typically be used in three dimensions.

Forced external convection can be controlled through a few means such as a rotating disk electrode, a flow cell electrode, or by bubbling a gas through the solution as demonstrated in Figure 12.^[113,114] The rotating disk electrode functions by creating a vortex current in the solution constantly drawing new electroactive material to the surface.^[114,118] This is achieved by spinning the electrode around a point and using the surface interaction or capillary effect between the electrode and the fluid to drag the solution out to the edges of the electrode. As such the flow is manipulated to always flow toward the center of the electrode and then to be pushed out to the side and then down in a standard convection flow cell.

A flow cell electrode functions by creating a laminar flow past the electrode. In turn this creates a similar effect to that of the rotating disk electrode but can also be paired with special electrodes with particular lattice orientations to allow for better film growth.^[114,116] The film can be manipulated to grow in a certain direction as the flow is unilateral, and as such can aid in the growth of certain structures if different variations in crystal lattice structure are inherently possible.

Bubbling an inert gas, such as Ar or N₂, through the system is another method to control the convection current by creating a larger offset current.^[113,114] This method is less accurate than the previous electrode flow-based methods, though it is perhaps more convenient to perform. If the rate of gas flow is controlled, then the convection current will be more consistent, though not necessarily measurable, or controllable. This causes disruption to the natural convection in a more consistent way and hence will allow for more consistent deposition that is not as precise as for the electrode methods.

Migration: Migration is the effect that is inherently controlled during electrodeposition. This is influenced by the external electric field that is applied across the electrodes. The ions are moved by the electric field toward the relevant electrode at a rate that is proportional to the field and the ionic mobility, u , as shown in Equation (10),^[114]

$$j_m \propto -u[B] \frac{d\phi}{dx} \quad (10)$$

where j_m is the migratory flux, and ϕ is the external magnetic field.

Although migration is controlled by the electric field applied, it is not ideal to have occurring in the solution. It will affect the rate of deposition as there is charge exchange at the electrode affecting the electric field and therefore the migratory flux and eventually the deposition rate, due to the extinction of charge in the solution.^[113,114] This can be controlled through the addition of a background electrolyte to allow for the charge exchange to occur in that material rather than the required deposition material. Increasing the background electrolyte to too high a proportion can also affect the deposition rate by limiting the movement of the desired charges, so it must be used in limitation.^[114]

A similar situation will also occur at the Helmholtz double layer.^[113,114] This is a model of the charge density near the electrode which suggests that as ions are deposited on the surface, the relative charge of the electrode will change and there will be a different potential at the surface than previously.^[113,114] Due to this effect, the deposition rate will be less consistent and will change over time as more charges are attached to the electrode. This theoretically will limit the overall thickness achievable by some materials through EPD as the potential could drop to a level that does not permit deposition. In practice, this effect can be helpful in deposition as a slowing barrier before impact at the electrode, by lowering the potential in direct proximity to the electrode, the ions will slow down before the impact on the substrate, lowering the energy of impact and increasing the sticking factor of the system.^[114]

Manipulating all of these different forms of mass transport is the key to achieving high quality EPD of materials, though there is still an inherent random nature to the processes that occur. There are more methods of manipulating these modes of transport than have been mentioned, but these are the most commonly used.^[113,114]

4.4.2. Thin Film Formation in EPD

The way in which the thin films form can be very different dependant on the size of the particles, the concentration of the solution, the structure of the end products, and the voltage across the circuit. Each of these will impact the film growth to form either in Volmer-Weber style, Stranski-Krastanov style, or Frank-van der Merwe style.^[121,122,123,124]

Volmer-Weber growth occurs when there are too few nucleation sites, so there are a small number of larger islands that are uneven in size and shape.^[122,124] Volmer-Weber growth occurs



Figure 13. Different types of thin film growth, A) Volmer-Weber, B) Stranski-Krastanov, and C) Frank-van der Merwe. It can be seen that the incoming particles (yellow) interact with the substrate (grey) and form either films or islands depending on each growth method.

when the attraction between ions is greater than the attraction to the substrate, meaning that the ions clump together on the substrate as shown in **Figure 13A**. This leads to a poor thin film with lots of discontinuities and defects and is generally not an ideal form of film growth. However, there are some uses for this form of growth in the construction of nanostructures on devices.^[124]

Stranski-Krastanov growth is the ideal case for thin film growth, known also as layer by layer growth.^[122,123] It occurs when every point on the substrate is a nucleation site simultaneously so there is a homogeneous thin film formed as shown in **Figure 13B**. This means that the film grows from every point on the substrate, and as such will be ideally spaced for the film structure, typically a lattice of some form. Stranski-Krastanov growth is very difficult to achieve and can be very useful even to approach, as it can be used to form monolayers.^[116,122,123]

Frank-van der Merwe growth is a hybrid of the two other types and is typically the most commonly observed form of growth.^[121,122] This is a practical hybrid of the two modes that observes both methods of growth, both thin film and island, in conjunction with each other as shown in **Figure 13C**. As such, the film is mostly homogeneous, though has some irregularities, that become exponentially more irregular as the thickness of the film increases.

In EPD Frank-van der Merwe growth is most typically seen, though this can be modified with the use of special flow systems to encourage particular growth methods as previously discussed.^[116] This is the case as there is an inherent chance of a particle depositing in a particular area, and once that particle has been deposited the chances of depositing next to it or on top of it are changed. In an ideal system, the deposited particles would not change the potential for other particles to be deposited, though this is very unlikely, and this is typically achieved by changing the potential across the system or changing the electrode. Generally higher concentrations, smaller electrodes, higher potentials, and similar Zeta potential for the material and the electrodes equate to shifting the growth mechanism toward Stranski-Krastanov.^[113,114,116]

4.4.3. Mass Transport at the Electrode

At the electrodes mass transport is slightly different than in the majority of the solution. To summarize all of the mass transport methods into one coherent model of movement, use **Figure 14** to visualize the motion of particles at the electrode. Starting at no bias and with no concentration gradient, the velocities of the particles are random. As a bias is applied, there is some movement of charges in the direction of the bias, and a concentration gradient appears due to this movement of charges. As the charged ions collide with the surface of the substrate, some are adsorbed onto the surface, which causes a buildup of charge at the interface between the solution and the substrate. As a full layer is deposited the charges of the electrode are somewhat blocked by the charges of the ions adsorbed to the surface, the Helmholtz double layer, which affects the concentration gradient negatively, slowing the rate of movement toward the substrate in the close vicinity of the substrate.^[113,114] This effect is combined with the natural motion and convection of the solution near the substrate, and the two effects reach a point where they start to cancel each other out, and a dynamic equilibrium is reached.^[114]

Depending on the size of the electrode, different assumptions can be made about how particles move in the electric field. The main assumption made is that the field lines are parallel, and the electrode is a planar source, however, at a range of $\approx 10 \mu\text{m}$ or below this assumption starts to fail and the field has to be assumed to be radial.^[113,114] These are referred to as microelectrodes. This affects the flow of the particles in solution and complicates calculations. However, microelectrodes have many benefits, the main benefit being the current flow is much lower than for conventional electrodes.^[113,114] This dictates the thickness of the diffusion layer, so for microelectrodes the diffusion layer is much thinner, and the diffusion gradient is much steeper, increasing deposition rate. This can be useful for increasing the number of nucleation sites on a substrate creating a smoother film by approaching Stranski-Krastanov growth.

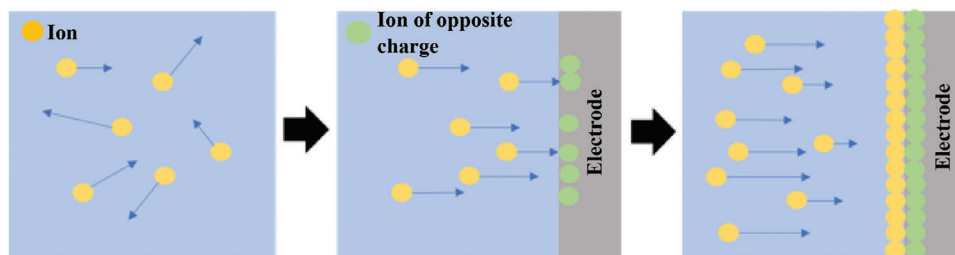


Figure 14. The process of applying a bias across the electrodes for mass transport. Charges in yellow and green are of opposite polarity. The length and direction of the arrows are indicative of motion and velocity.

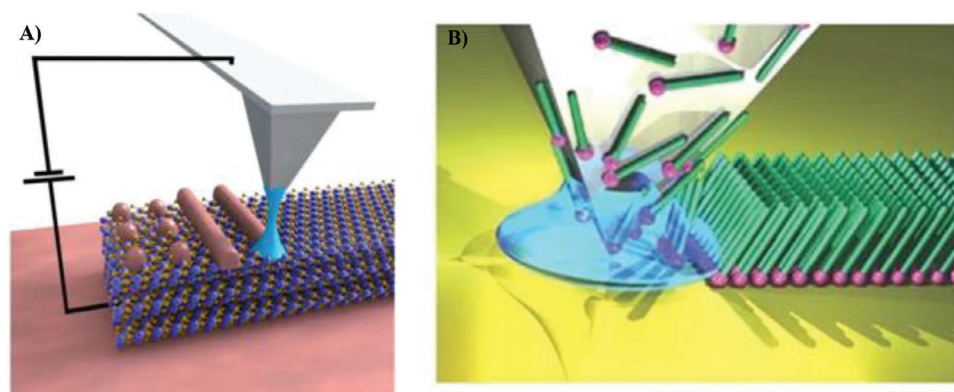


Figure 15. Demonstrations of SPL using A) an oxidation method to create dots and lines from Reproduced with permission.^[154] 2017, IOP. and B) an ink deposition method from Reproduced with permission.^[126] 2007, Springer Nature showing orientationally dependent deposition.

4.4.4. Electrochemical Patterning

Electrochemical patterning is another potentially very useful area to use for the fabrication of PD devices. This process essentially uses either an electrode design that is already patterned or manipulates the electric field between the electrodes to pattern the device.^[18,125]

One of the easiest methods is to pattern the electrodes prior to EPD, which can typically be done through thermal evaporation, sputtering, or photolithography.^[54–56] Using these methods combined with the already well-established techniques from evaporation, sputtering, and photolithography which can pattern high-resolution devices with ease, with the ability to deposit solely on the electrodes from EPD. Due to the nature of EPD, the deposition process tends to happen on the conductive parts of the electrodes which allows for highly pixelated and patterned devices through the use of EPD similar to the effects of the previous methods mentioned.^[18,19] However, this still uses the already established methods for deposition of the electrodes and is not the most effective use of EPD.

Another method is using direct writing electrochemical lithography, more commonly known as Scanning Probe Lithography (SPL).^[61,62] This uses a small conductive tip to trace a pattern over an electrode that has been coated in a solution containing the required deposition material shown in **Figure 15**. As the tip moves over the surface, a current is passed between the tip and the electrode passing through the solution, allowing the reaction to occur in a small area direct line between the tip and the electrode. This can then be used for subsequent depositions by changing the solution that sits on the electrode surface. Alternatively, the solution can be an ink that is dropped from a nozzle that is electrically charged, provided that contact is maintained between the electrode of the nozzle and the substrate at all times.^[125,126] This method can also be carried out using the equipment for Atomic Force Microscopy (AFM) by passing a current through the AFM tip as it taps across the surface or through Scanning Tunneling Microscopy (STM) through a similar process.^[127–130]

It is also possible to deposit material on a non-conductive surface if the non-conductive layer is thin enough on top of a conductive layer.^[69,131] This will allow for a tunneling current to pass through the non-conductive layer, and the potential difference

across the system can cause deposition to occur. This will allow for the deposition of base electrodes by EPD itself, allowing for a fully EPD-fabricated device. However, this has drawbacks in how to float the non-conductive layer off the conductive layer used as the electrode for deposition, as for the layer to be thin enough to carry this out, the layer would lack integrity and be extremely delicate.

5. Organic Photodetectors and Image Sensors

As mentioned previously, organics are a good material for use in PDs and image sensors and have been used extensively both in research and industry. They are typically safe for consumer usage though they can be unstable for long-term performance.^[12,77] OPDs can be split up into two main focus areas, broadband PDs, and narrowband PDs, for use either with or without external filters respectively. Both areas have vastly different uses from medical to everyday photo taking, so the wide range of organic semi-conducting materials allows for tailor made PDs for each specific circumstance.^[2]

5.1. Broadband OPDs

The operational detection range of OPDs is typically decided by the absorption spectra of the organic materials in the PA layer as stated previously.^[2,30,132] However, the EQE can be affected by other areas of the device structure. To achieve truly spectrally broadband OPDs, either a combination of different organics must be used, or the device structure must be altered.

When discussing a truly spectrally broadband PD it is implied that the response would be roughly the same across a wide spectrum of wavelengths. Some organics inherently have this absorption profile, and some have peaks that align conveniently with the peaks of other organics to create more smooth spectra. However, this will still lead to some difference in output current from the PD device. The main methods to achieve the aim of a truly spectrally broadband PD include device structure alterations. These structure alterations include adding optical cavities into the device using semi-transparent electrodes or increasing the thickness of the junction in the device. The idea behind including optical cavities in the device is to increase the Q-factor by partially

reflecting the incident light on the electrodes.^[95] This would allow for tuning of the absorption and EQE. Changing the junction thickness would achieve a similar effect to this by changing the shape of the EQE spectra.^[30]

A benefit of using organics in PDs is that they have wide absorption ranges and as such can be used for UV-Vis-NIR PDs. These types of PD can be used for many different situations, though in industry are typically used in tandem with filters to create narrowband detectors.^[133] The reason for using these wide range PDs is that they tend to be more stable and have higher detectivity and responsivity over wider ranges of input wavelength. As such, when used with a filter, they can be more efficient to use than inherently narrowband devices.

Recently, very high detectivities of $\approx 10^{14}$ Jones have been reported for OPD devices in shorter ranges, however, in wide range OPDs the detectivity is more commonly found to be $\approx 10^{13}$ Jones.^[2,3] Though this is not necessarily indicative of progress, it has mainly been finding methods of increasing the detectivity with future materials in mind. This has typically been done by lowering the dark current density in the devices through various different means. One method has been to include a composite hole blocking layer in the PA layer as shown by Xu et al.^[134] and Li et al.^[135] These have peak detectivities of 2.3×10^{13} Jones and 4.2×10^{13} Jones respectively, but they have successfully lowered the dark current density to 1.2 nAcm^{-2} and 0.18 nAcm^{-2} . This was done by essentially blending the PA layer with a hole-blocking layer to suppress the reverse injection of the devices.

The bandwidth of these devices is the other most important quality, with devices ranging from 300 to 1450 nm as shown by Gong et al.^[132] Increasing the bandwidth can be done mainly by changing the materials used in the PA layer, or by blending them together. Gong et al. blended poly(5,7-bis(4-decanyl2-thienyl)-thieno(3,4-b)diathiazole-thiophene-2,5) PDDTT with PC₆₁BM to achieve the wide range.^[132]

5.2. Narrowband OPDs

One of the main issues with PDs and image sensors is the ability to target specific wavelengths for absorption. Most image sensors lack this ability and require bulky filters to block certain wavelengths to allow for purer color detection. As such, this is an area that is very important, particularly as the idea of flexible devices is becoming more prevalent. The most common approach to achieve the removal of filters is to take a material-based approach.

5.2.1. Charge Collection Narrowing (CCN)

One recent method that has been used to create unfiltered narrowband photodetectors is a phenomenon called Charge Collection Narrowing. This is an effect proposed by A. Armin and P. Meredith where the thickness of the photoactive layer can impact the absorption profile of a PDD device.^[30] They claim that a thicker layer can create an electrically and optically thick junction, which allows for a decrease in the bandwidth of the detector increasing color resolution. This occurs due to the nature of the absorption profile of the materials used and

the structure of the PDD device, as shown in **Figure 16**. Higher energy photons are preferentially absorbed when incident on the PA layer, which means that the higher energy photons are absorbed closer to the incident surface. In a thick layer, this means that the time taken for the electrons and holes to reach their respective electrodes is different, lowering the efficiency at those wavelengths. As such, the performance of the device increases as the wavelength gets closer to the absorption onset, and if the effect is pushed to the limit, then a narrowband PDD device can be achieved. PCDTBT:PC70BM and poly[2,5-(2-octyldodecyl)-3,6-diketopyrrolopyrrole-alt-5,5-(2,5-di(thien-2-yl)thieno [3,2-b]thiophene)] (DPP-DTT):PC70BM were used as the PA layers to achieve this CCN effect for IR and red color selection respectively.^[30] The reported FWHM is $<90 \text{ nm}$ for both devices and was the first truly narrowband ($<100 \text{ nm}$) OPD, with the detectivity being $\approx 10^{12}$ Jones for both devices.^[30]

5.2.2. Internal Light Depletion (ILD)

Another method is to use ILD. This is achieved by adding a depletion layer into the device to absorb in very similar regions to the main PA layer, however, due to the short diffusion length of the excitons formed in the depletion layer, they cannot reach the interfaces required for current flow.

This has been demonstrated by Wang et al.^[75] to show a narrowband peak of 60 nm FWHM centered $\approx 760 \text{ nm}$ with a peak detectivity of 10^{13} Jones. It was done by using P3HT:PTB7 as the depletion layer on top of an ITO/PEDOT:PSS layer, a separating layer of PBTTT and then a PA layer of PM6:IT4F with Al as the top electrode shown in **Figure 17A**.^[75] By choosing two organics with similar absorption spectra and using one to filter the light to the other, a thin film filter has been made integrated into the device.

Using a similar idea Suman et al.^[136] created a TiO₂-based detector using the narrowband nature of Squaraine as a depleting layer for the TiO₂ combined with ZnO to solely allow for absorption of red light in the device. The FWHM is quite large at 116 nm around a center of 650 nm with a detectivity of 2.57×10^{10} Jones.^[136]

5.2.3. Charge Injection Narrowing (CIN)

A final standard approach to narrowband OPDs is to use CIN. This is similar to CCN though adds a large bias across the PD to enhance the effect of the narrowing in one direction. Introducing the bias across the PD allows for photomultiplication which increases the injection of charge carriers in the PD. When combined with the CCN effect, this will affect the optimized wavelengths more and make the effect more prevalent, and also increase the efficiency of the device. It is important to note that the direction of the device is more important in this case, as switching the direction of the bias changes the flow of charges decreasing overall efficiency and creating a broader spectrum of detection.

This has been shown by Jiao et al.^[89] using a $2.8 \mu\text{m}$ thick blended layer of P3HT:PC₇₀BM, to achieve a 9.73×10^{13} Jones detectivity at 650 nm with a 40 nm FWHM. From **Figure 18A** it

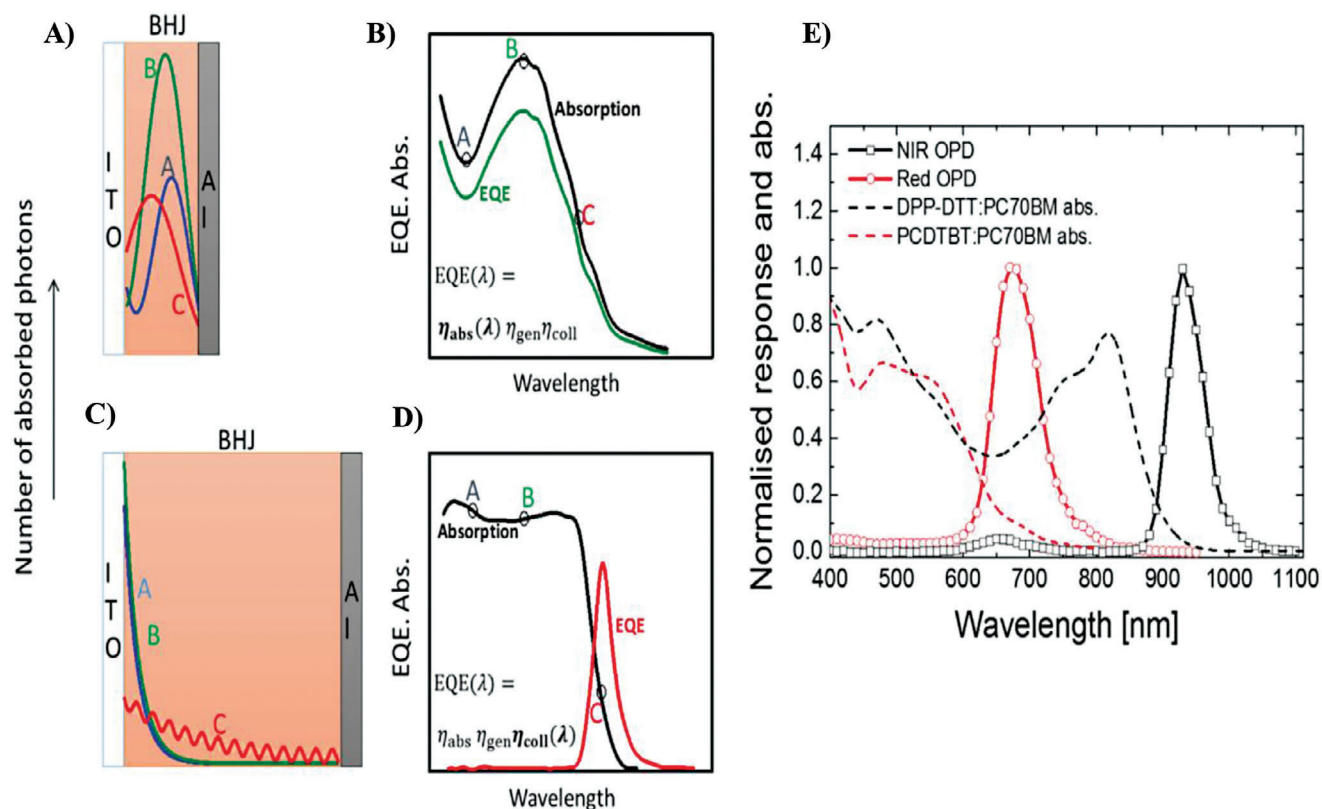


Figure 16. The effects of CCN found by Armin et al. Reproduced with permission.^[30] 2015, Springer Nature. showing, A) and B) the absorbed photon distribution for a thin and thick junction device respectively, C) and D) the absorption and EQE of the thin and thick junction device respectively, and E) the effects of the final devices with CCN active.

can be seen that adding a 0.8 nm thick layer of Al_2O_3 between the PEDOT:PSS, and P3HT:PC₇₀BM layers decreased the dark current density by a factor of ≈ 10 .^[89]

Liu et al.^[76] used a similar method using a ternary blend of P3HT:PTB7-Th:BEH with a PEDOT:PSS HTL sandwiched be-

tween ITO and Al demonstrated in Figure 18C. This led to a FWHM of 27 nm centered ≈ 850 nm and a peak detectivity of 8.8×10^{11} Jones at a bias of -13 V.^[76] The CIN method is one of the most promising sources of narrowband detectors, however, it has the drawback of requiring high biases. In this case, the high

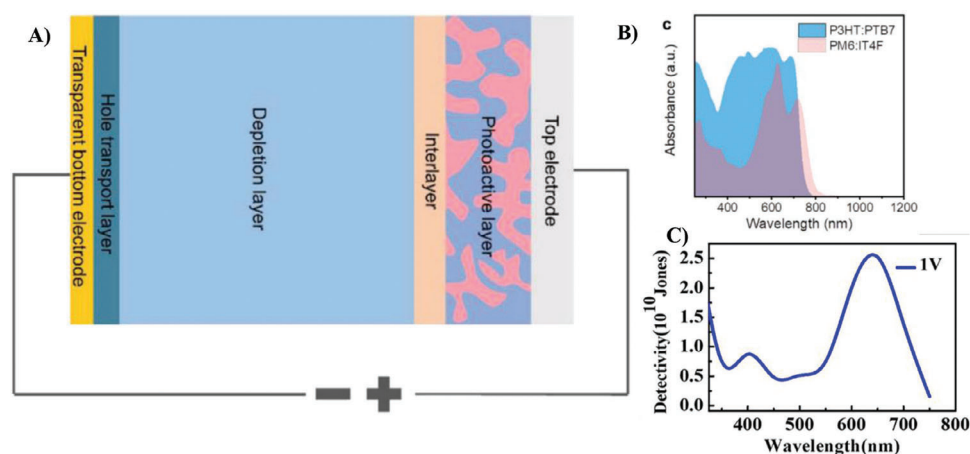


Figure 17. Internal light depletion A) device structure from Wang et al. Reproduced with permission.^[75] 2023, John Wiley and Sons. B) idea demonstrated by overlapping absorption spectra from Wang et al. Reproduced with permission.^[75] 2023, John Wiley and Sons. C) detectivity of Squaraine TiO₂ detector from Suman et al. Reproduced with permission.^[136] 2023, American Chemical Society. It can be seen in B that the overlap of absorption is significant and should give rise to a narrowband absorption peak when combined.

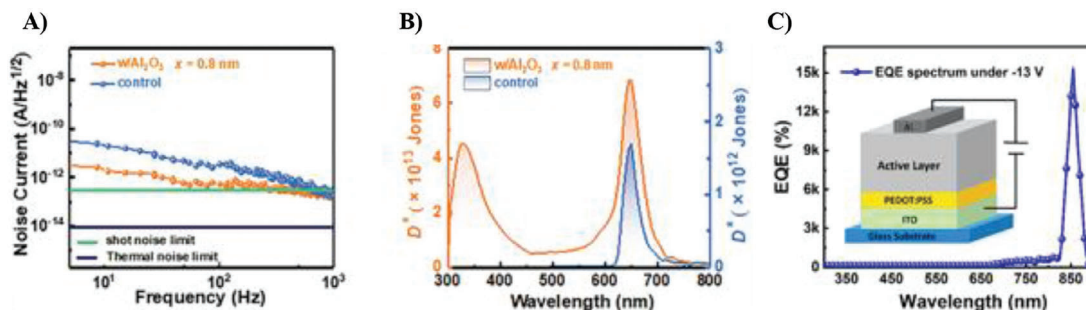


Figure 18. Charge Injection Narrowing A) demonstrating the effect of Reproduced with permission.^[89] 2023, John Wiley and Sons. adding the Al₂O₃ layer on the dark current density, B) the effect of changing the bias direction on device performance from Reproduced with permission.^[89] 2023, John Wiley and Sons. C) the EQE of Reproduced with permission. 2022, Springer Nature. with the ternary blend device. Reproduced with permission.^[76] 2021, American Chemical Society.

bias also massively increases the EQE due to photomultiplication effects taking place within the diode with an EQE of 15300%.^[76]

5.3. Organic Image Sensors

Organic image sensors are a promising area for many different reasons. One benefit of using organics over conventional structures is that the inhomogeneity of the films and lack of rigidity allows for easier fabrication of flexible image sensors.^[2,15] The ability of most organic molecules to flex and bend to some degree make them preferable to crystal structures for the purpose of flexible devices. This combined with the ability to produce large area devices through solution processing methods allows for the fabrication of many different devices ranging from medical biosensors to RGB cameras.^[2,3]

Inkjet printing as a method of fabrication has been used more frequently with the intention of fully printed devices. Eckstein

et al.^[15] achieved a fully printed OPD array of 256 individual pixels of area 250×300 μm shown in **Figure 19D**. The device was a simple PD structure of Ag/ZnO/PTB7:PC₇₀BM/PEDOT:PSS, each layer was sequentially inkjet printed inside a bank structure of SU-8 photoresist. This bank structure is typically used to allow for easier pixelation control in printing to control the drop area more accurately. The detectivity of the device was recorded ≈10¹² Jones, with a LDR of 114 dB clearly seen in **Figure 19E**.^[15]

A broadband image sensor was produced by Wu et al.^[137] using a two-terminal approach. The device structure of ITO/PEIE/P3HT:PCBM/PEDOT:PSS/P3HT/NaF/Al, using two PA layers separated by a HTL layer.^[137] This allows for the device to have a large responsivity upward of 40 A W⁻¹. An 8×8 array of 500×500 μm pixels was fabricated by patterning the ITO and Al into strips allowing for each pixel to be a vertical stack that could be distinguishable through direct measurement instead of signal processing. This would decrease the imaging time, providing an image potentially faster, dependant on the size of the array.

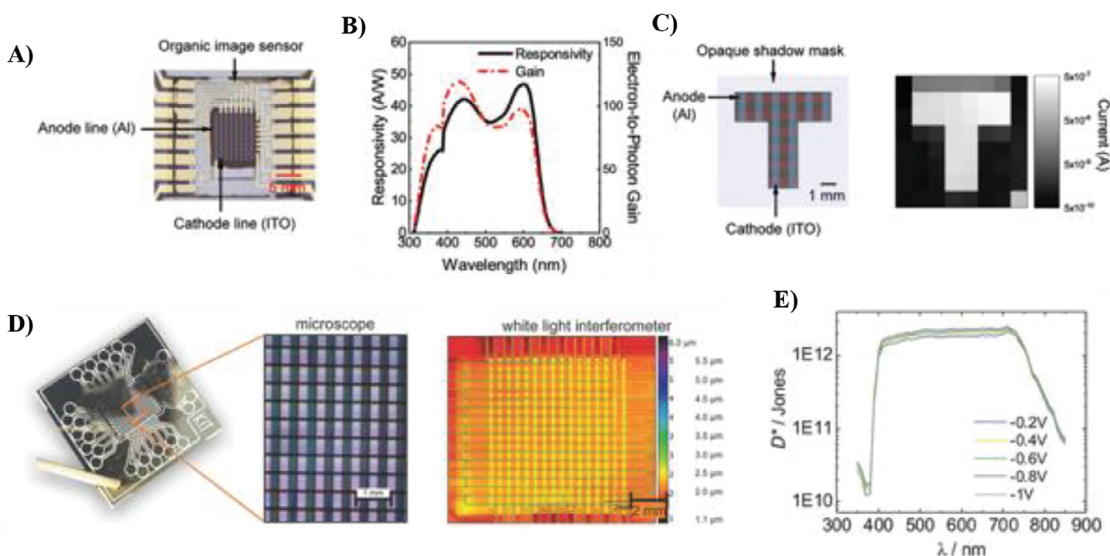


Figure 19. A) Image of device fabricated by Wu et al. Reproduced with permission.^[137] 2019, John Wiley and Sons. B) a representation of the response from Wu et al. Reproduced with permission.^[137] 2019, John Wiley and Sons. C) a test of the pixelation accuracy of the device illuminated through a shadow mask from Wu et al. Reproduced with permission.^[137] 2019, John Wiley and Sons. D) images of the device fabricated Eckstein et al. Reproduced with permission.^[15] 2018, John Wiley and Sons. under microscope and white light interferometer, E) detectivity of the device from Eckstein et al. over the operational wavelength range. Reproduced with permission.^[15] 2018, John Wiley and Sons.

6. Quantum Dot Photodetectors and Image Sensors

QDs have many properties that put them above other material types to be used in photodetectors and image sensors as discussed in Section 1.5. As such they have been used extensively in research and in industry both for display and detection purposes in narrowband detectors.^[11] As broadband detectors QDs can often struggle and require much more additional device restructuring. However, despite the benefits of QDs, the QDs that have been used in industry are typically toxic heavy metal based, either lead or cadmium. This is not ideal given the close contact that humans have with these devices, so research is being carried out for safer, less toxic replacements to achieve the same performance.^[138]

6.1. Narrowband QPDs

QPDs have similar methods of achieving narrowband functionality, though some areas are more intuitive due to the inherent absorption of QDs. The narrowband absorption of QDs results in less need for manipulation to achieve a narrowband PD device.

The most prevalent QD used in QPDs is Lead Sulphide (PbS). This is mainly due to the high confinement factor, which allows for higher performance in general, though PbS is also significantly more stable in air than most other QDs which means it is easier to work with and use in devices instead of requiring a different atmosphere. However, PbS is generally focused in the NIR range, so it has limitations on its use.

The idea of ILD can also be applied to QPDs as shown by Qiao et al.^[139] used two types of PbS to fabricate a narrowband QPD by stacking two different sizes on top of each other with a blocking layer in between the two PA layers. The device was setup as a PC with only one layer of 1120 nm PbS QDs between two gold electrodes, topped with a thin layer of poly(methyl methacrylate) (PMMA) to act as a charge blocking layer, and capped with a layer of 980 nm PbS QDs seen in Figure 20E.^[139] The shorter wavelength QDs act as a thin film filter for the device achieving a FWHM of ≈ 100 nm which could be tuned to be smaller by changing the size of the QDs further. As stated previously this method has limitations due to the loss of light, though for use as a narrowband PD it is a simple and robust method.

Much the same as in OPDs, using blocking layers can also increase the detectivity of QPDs. Ma et al.^[140] showed that by inputting an 18 nm layer of PMMA in between the ETL and PA layer, they could decrease the dark current by a factor of ≈ 10 and increase detectivity to 4.01×10^{13} Jones at a low bias of -1 V.^[140]

Changing the ligand on QDs has been shown to have a large impact on the properties of the QD. This makes sense as the surface chemistry of the crystal changes and the majority of the atoms in the particle are at the edges due to the size of the QD. As such, changing the ligand can be used in many different ways to affect the performance of the device. Bothra et al.^[80] performed a study seen in Figure 20D on the effect of different ligands on the performance of PbS based PDs, using lead halide ligands, Methylammonium Lead Iodide (MAPbI₂), and Caesium Methylammonium Formamidinium (CsMAFA) ligands.^[80] It was found that

using the different ligands would change the EQE spectra, shifting peak position due to bandgap differences, and that the dark current was drastically reduced in the lead halide ligand to 5 nA at -0.2 V.^[80] These are not strictly speaking narrowband QPDs, though it is important to note the effect of changing the ligand on device performance for future work.

Another group of QDs that are commonly used is Cadmium Selenide (CdSe) or Cadmium Sulphide (CdS). Again, these QDs have strong confinement so are ideal for high performance devices. These QDs tend to be based in the RGB range potentially making them useful for RGB image sensors.

Kalsi et al.^[65,141] doped CdS QDs with copper to attempt to change the absorption properties of the QDs. It was found that by doping 4% copper the detectivity could be increased to 1.12×10^{14} Jones with an EQE of 5080% at 782 nm using a M-S-M device structure of Ag/CdCuS/Ag.^[65] This is similar to the previous work carried out on magnesium doped CdS QDs where a detectivity of 3.45×10^{13} Jones was achieved.^[65]

The final group of QDs are the newer “safe” QDs such as Indium Phosphide/Arsenide (InP/As) or Copper Indium Zinc Sulphide/Selenide (CIZS/Se). These QDs are far less toxic and can therefore be used in a commercial capacity more easily, though they are less well confined and are typically less efficient.

Using InP/ZnS in a PDD structure Nemoto et al.^[66] were the first to achieve a device with detectivity of 8×10^9 Jones at 470 nm using a structure of ITO/ZnAlO/InPZnS/Al.^[66] This is one of the first non-toxic PD devices fabricated, and it was done using ligand exchange on blue InP to increase the efficiency shown in Figure 20A,B. It was found that switching ligands from Oleylamine to 6-mercapto-1-hexanol improved the quality of the QD film formed for devices.

It is important to note that most of these “safe” QDs are shelled, that is to say that they have a thin outer layer of a different crystal structure, typically Zinc Sulphide (ZnS), that allows for smoother interactions between quantum dots. They are both chemically and photonically isolating depending on their thickness, which can be used to different effect in emitting and detecting devices. Removing this shell lowers the stability of the QD and can lower the quantum yield, although it can also improve the device performance in detecting devices by increasing the packing factor and allowing for better charge transport through the QD layer, one of the major limitations of using QDs. Changing the core-shell structure can also change the response time as shown by Peng et al.^[90] Using a core-shell structure of InSb/InP, it was possible to achieve a detectivity of 4.4×10^{11} Jones and a response time of 70 ns demonstrated in Figure 20C.^[90]

Another use for QDs is in PT based devices. Detectors based on this structure have the benefit of changing the voltage across the detector to achieve different efficiencies in device performance, such as an increase in detectivity or responsivity. This is demonstrated by Zhan et al. in their use of perovskite based quantum dots to create a blue sensitive PT device.^[142] Using Caesium Lead Halide perovskite QDs deposited on a channel layer of IGZO and allowing for the removal and changing of ligands through Ethyl Acetate cleaning, a responsivity increase of ≈ 1400 was found by removing the ligands, leaving a responsivity of $\approx 5.4 \times 10^5$ AW⁻¹.^[142]

Using PbS QDs and nanowires respectively Pak et al.^[83] and Giraud et al.^[67] developed PT devices with fast response times

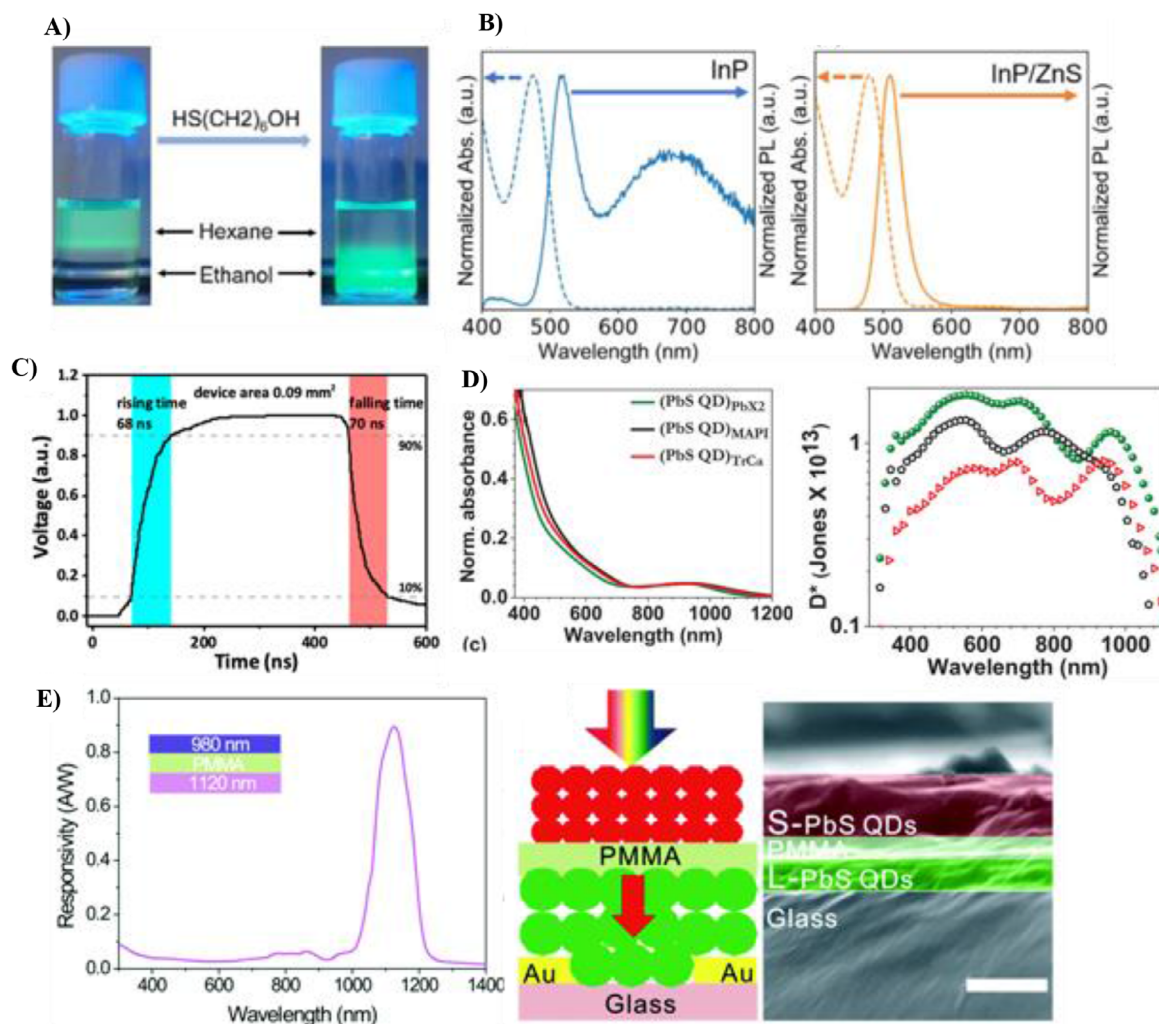


Figure 20. A) Demonstration of ligand exchange, changing the phase of the QDs by Nemoto et al. Reproduced with permission.^[66] 2023, Royal Society of Chemistry. B) absorption and photoluminescence of ZnS shelled and unshelled InP by Nemoto et al. Reproduced with permission.^[66] Royal Society of Chemistry. C) response time of the PD fabricated by Peng et al. Reproduced with permission.^[90] 2024, American Chemical Society. D) the effect of ligand exchange on the absorption and detectivity of device from Bothra et al. Reproduced with permission.^[80] 2022, John Wiley and Sons. E) the responsivity of the device from Reproduced with permission.^[139] 2016, Royal Society of Chemistry. and an SEM image of the side profile of the device with a structure diagram.

and high detectivity. Pak et al. fabricated a device using MoS_2 as the channel layer with PbS as the PA layer seen in Figure 21.^[83] In theory this increases the rate of charge transfer through the transistor allowing the charges generated to travel through the highly conductive channel layer as opposed to the relatively less conductive PA layer. As such this can decrease response times to $950 \mu\text{s}$ as found by Pak et al.^[83] Giraud et al. fabricated a PbS nanowire PT device and obtained a peak detectivity of 1.9×10^{13} Jones at a negative gate bias of $\approx -10 \text{ V}$.^[67]

6.2. QD Image Sensors

QD image sensors are an exciting new area of PD research, they have a lot of potential to be revolutionary in the area of image sensing due to their high efficiency and color accuracy. Due to the nature of QD films, it is also possible to make flexible detectors

and image sensors more easily than with conventional materials. For thin devices, QDs would lead the way, even over organics due to the high absorption and packing factor, leading to thinner films, which in turn will increase flexibility.^[142]

Liu et al.^[91] have recently produced a PbS based image sensor using a monolithic CMOS readout method, images from which can be seen in Figure 22A. It is a broadband image sensor in the NIR region with a wide range of 400–1300 nm, a detectivity of 2.1×10^{12} Jones, and a linear dynamic range of more than 100 dB.^[91] The spatial resolution of the sensor is 40 line pairs per millimetre. It was shown to be better than a standard InGaAs when comparing the grey levels between images.

An array of PT devices can be used as an image sensor as has been shown by Chen et al.^[138] in Figure 22C to be an effective method for image detection. Using CIZS QDs combined with a layer of InGaZnO in a 5 by 5 transistor array. The structure was such that the InGaZnO was used as a dielectric layer and

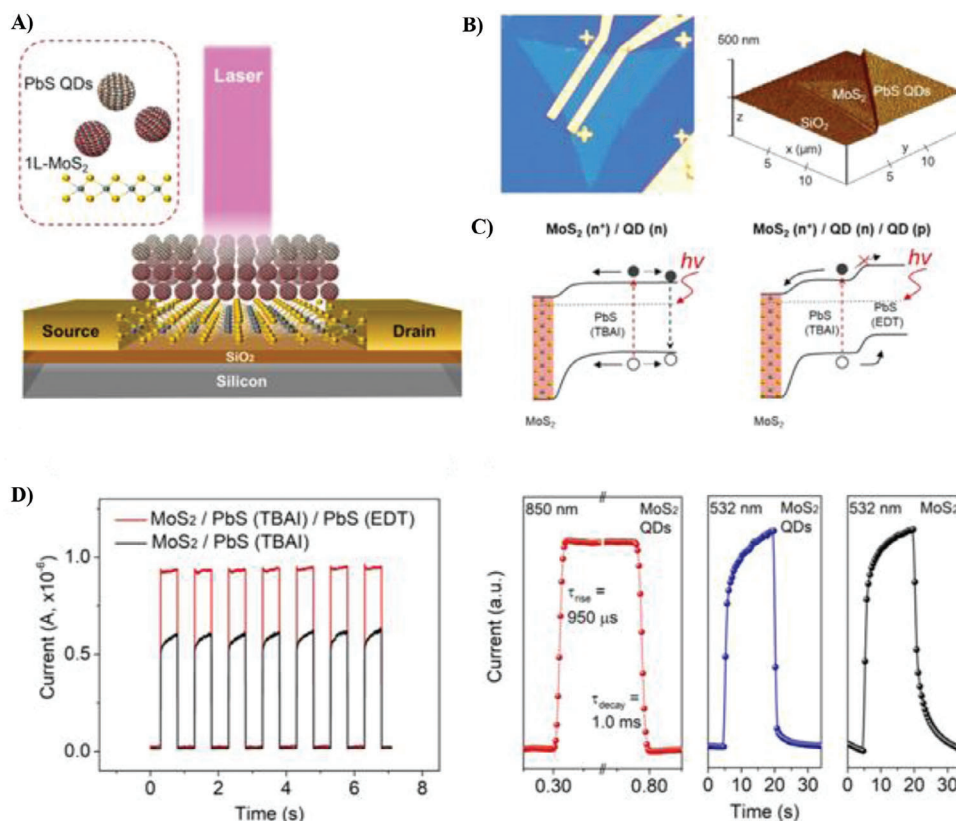


Figure 21. A) Depiction of the structure of devices fabricated by Pak et al. Reproduced with permission.^[83] 2018, American Chemical Society. B) Microscope and AFM image of device showing single MoS₂ crystal from Pak et al. Reproduced with permission.^[83] 2018, American Chemical Society. C) Bandgap structure for PT device from Pak et al. Reproduced with permission.^[83] 2018, American Chemical Society. addition of an extra layer of doped QDs prevents charge transfer in the wrong direction. D) Temporal response of the photocurrent with illumination at 850 nm and zoomed in to show response time with excitation above and below the absorption of MoS₂ from Pak et al. Reproduced with permission.^[83] 2018, American Chemical Society.

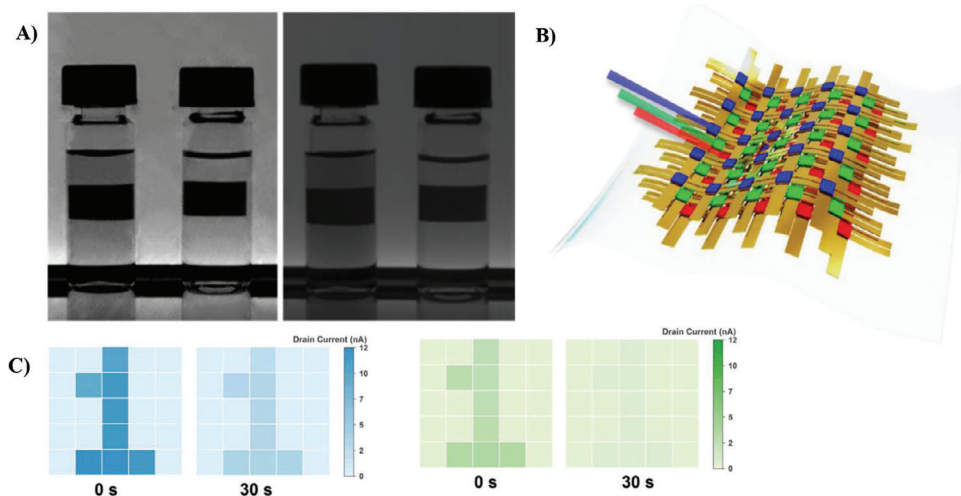


Figure 22. A) Image of two filled vials taken by the PbS image sensor of Reproduced with permission.^[91] 2022, Springer Nature. compared to an image of the same two vials taken by a commercial InGaAs image sensor. B) Representation of the device fabricated by Reproduced with permission.^[143] 2022, Springer Nature. with the flexible nature of the device apparent. C) Demonstration of the memory effect of the PT array developed by Chen et al. Reproduced with permission.^[138] 2024, John Wiley and Sons. under blue and green illumination respectively.

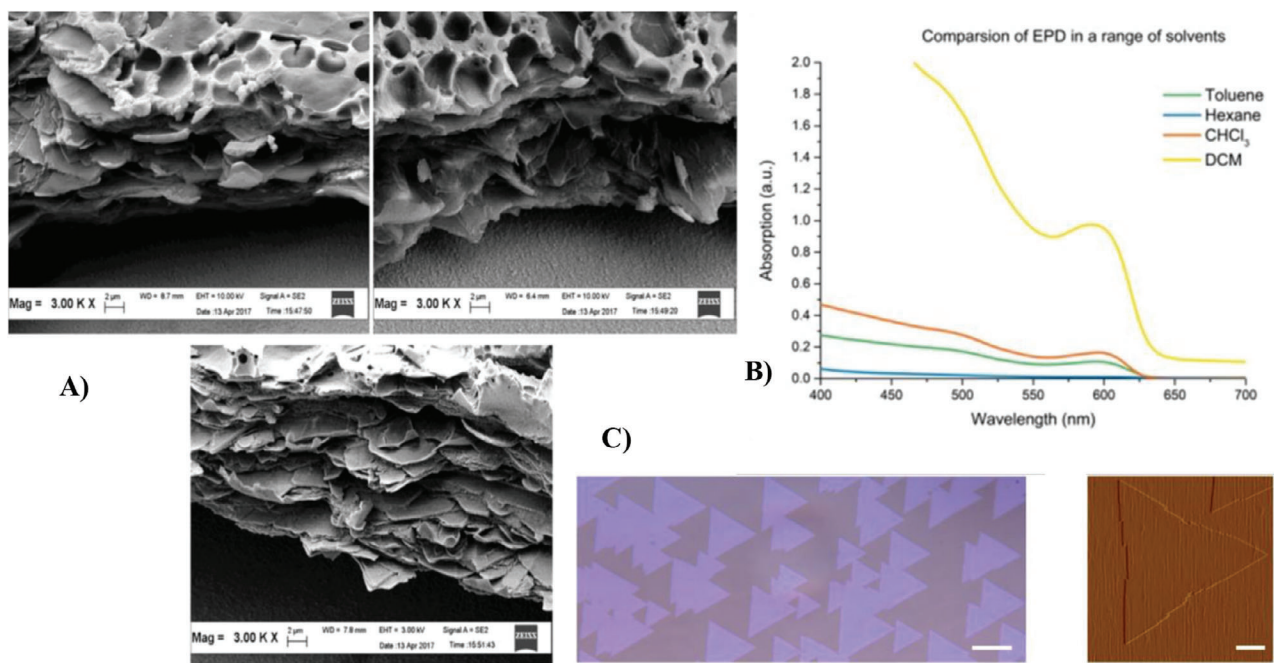


Figure 23. A) SEM images of the CdSe film electrochemically deposited by Reproduced with permission.^[145] 2022, Springer Nature. B) absorption of CdSe films after EPD using different solvents for the process from Reproduced with permission.^[115] 2019, MDPI. C) microscope image and AFM image of MoS₂ single crystals grown through EPD by Reproduced with permission.^[116] 2021, Springer Nature.

the CIZS QDs were the PA layer. The peak detectivity was high at 3.4×10^{15} Jones with a working range of 480–630 nm.^[138] It was used to create a synaptic memory effect in the sensor with images still visible 30 seconds after illumination with a $2 \mu\text{W}$ light source.^[138] An image sensor such as this could be used as a type of short term memory storage device among many other uses.

Another potentially useful property of an image sensor is to be flexible and stretchable, which would increase the number of scenarios that the image sensor would be functional in. Song et al.^[143] developed a $5 \times 5 \times 3$ PT flexible and stretchable array for RGB color detection using CdSe QDs shown in Figure 22B. This was achieved by blending the QDs in with a semiconducting polymer, PDPP2T, to allow for the stretching of the structures and fabricating a series of interweaving fibres with pixels located at regular intervals throughout. These were spin-coated and deposited onto a layer of SEBS to allow for better flexibility and stretching. Despite the innovation in the device structure, device performance suffers dropping the detectivity to 3.8×10^6 Jones.^[143] It is suggested that the device performance could be improved by applying a higher resolution patterning to the active device area.

7. Potential Electrochemical Methods for PDs

Many different types of material can be used to deposit electrochemically onto a surface, the only requirement is to have a charge associated with the particles that are desired to be deposited. These materials can range from organics, to QDs to various TMCs and metal oxides. Alternatively, metal oxides can be formed on a surface through reduction or oxidation allowing for a wide range of different possibilities using electrochemistry for this area.

Though electrochemistry is not typically used in the fabrication of PD devices, it has been used in very similar areas and the same steps and ideas can be applied to these circumstances. Bulk TMCs are typically easier to deposit using this method than organics or QDs as they require less fine tuning to achieve a high quality functional layer.

The advantages of EPD over other standard methods are that it is usually cheaper and quicker. For example, Chemical Vapor Deposition (CVD) and thermal evaporation are commonly considered the two highest quality methods of crystal growth or formation, but recently EPD has been used to form large scale single crystals of TMCs that almost rival the quality of CVD at a fraction of the cost as shown by Li et al.^[116] By using an electrochemical flow cell in the direction of the C/A plane in a cut sapphire crystal Li et al.^[116] were able to produce a large area (50 mm) single crystal of MoS₂ as seen in Figure 23C. This was then used to create a field effect transistor, though it could be easily modified to be used either as a PT or a PC through thermal evaporation of electrodes onto the surface of the crystal.

A similar method for deposition of TMCs was also used by Patel et al.^[144] in the EPD of MoSe₂ nanocrystals. The MoSe₂ nanocrystals were electrochemically deposited onto ITO and topped with an Ag electrode through thermal evaporation. This created a PC device with a detectivity of 3.69×10^{13} Jones.^[144] Using nanocrystals in this way is similar to using QDs, though the crystals are ≈ 35 nm in size, significantly larger than a QD. As such this method could easily be applied to QPDs.

Purcell-Milton et al.^[115] investigated the role that solvent plays in EPD of QDs, in particular Oleic Acid capped CdSe. Using a TiO₂ electrode and four different solvents, Chloroform, Dichloromethane, Toluene, and Hexane, the absorption of the films developed was taken as a measure of the thickness and

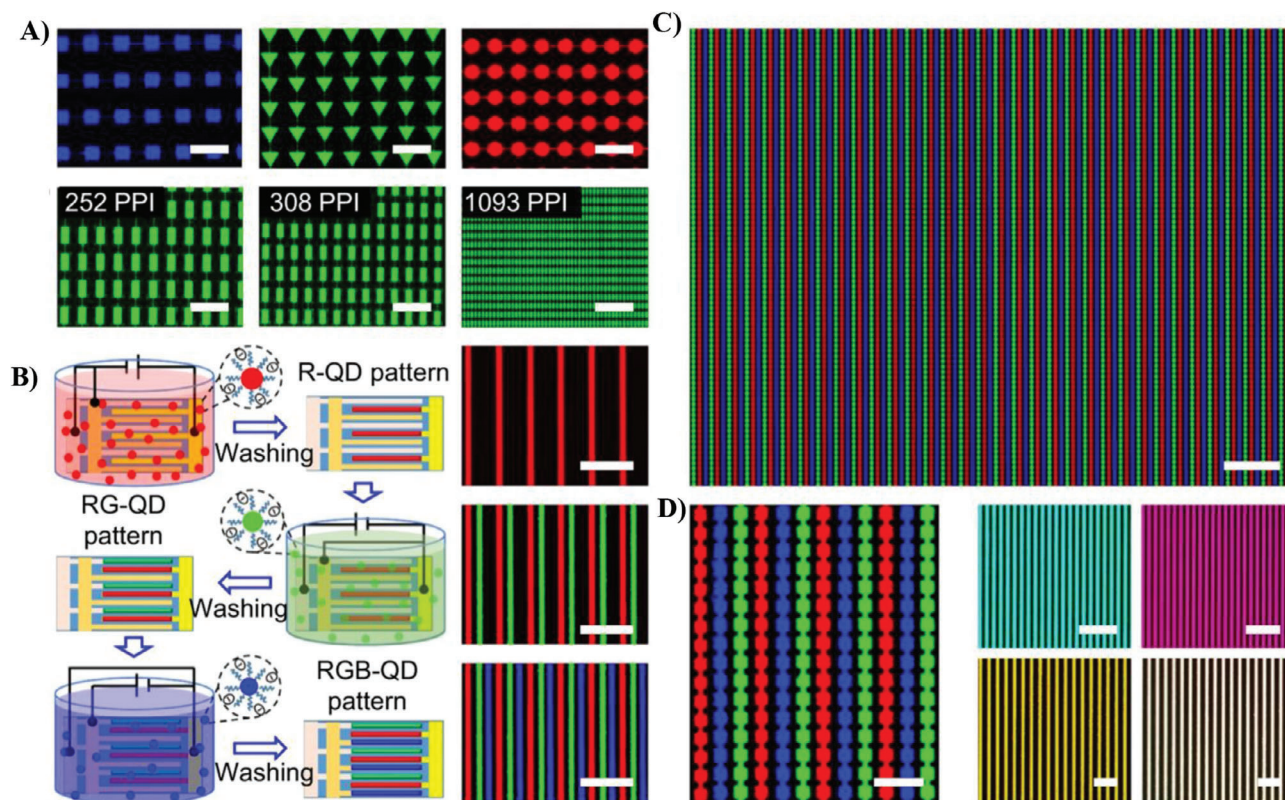


Figure 24. A) Demonstration of patterning using EPD on device fabricated by Zhao et al. Reproduced with permission.^[18] 2021, Springer Nature. B) the method used by Zhao et al. Reproduced with permission.^[18] 2021, Springer Nature. for the deposition of multicolored arrays using EPD, C) image showing the large area capabilities of EPD for device fabrication, D) demonstration of multicolor arrays developed by Zhao et al. Reproduced with permission.^[18] 2021, Springer Nature. to show cyan, magenta, yellow and white emission from RGB device.

density of the films produced. It was found that Dichloromethane was by far the best of the solvent choices due to the high dielectric constant of 8.93. With this high dielectric constant, the QDs would be preferentially drawn through the solution to the electrodes rather than the solvent, increasing the rate at which the film forms. The adhesion of the films to the TiO₂ electrode was high as only $\approx 20\%$ of the film was lost after cleaning in Dichloromethane.^[115]

Ishak et al. used EPD to deposit CdSe QDs for use in a solar cell as seen in Figure 23A,B.^[145] The ligands used on these quantum dots were changed to Trioctylphosphine Oxide (TOPO) and Mercaptoundecanoic Acid (MUA) and the QDs were suspended in Chloroform. Depositing for 5 min at 100 V onto FTO was found to give a relatively uniform film. It was found that as the size of the QD increased, the voltage required to deposit it uniformly also increased, regardless of the ligand used. Poulou et al. also deposited CdSe QDs for use in a solar cell, depositing instead onto TiO₂.^[19] CdSe QDs from a solution of Chloroform were used to produce a thick layer on the TiO₂ thin film, though the deposition was not entirely uniform.

CuInS QDs have also been used for the fabrication of solar cells using EPD, as shown by Santra et al.^[146] Again, FTO and TiO₂ were used as the electrodes in the system, with Chloroform as the solvent. However, the use of a safer, less toxic QD is promising as most other work has been carried out with toxic QDs, unsuitable for use in commercial cases.

Another area that is more relevant is in the fabrication of emissive layers using QDs. Zhao et al.^[18] used a combination of photolithography and EPD to achieve a high density QD array seen in Figure 24. By using ligand exchange to ensure that the QDs had a similar negative charge using polyethylene glycol (PEG-COOH) arrays of ITO patterned by photolithography. The ITO had a width of $\approx 2 \mu\text{m}$ and the pattern consisted of alternating lines connected to different electrodes.^[18] Using this EPD on this pattern allowed the deposition of RGB colored CdSe QDs onto the device by altering the voltage across the system between positive and negative when submersing the device in different QD solutions. This allowed for the QDs of one color to be drawn to one series of strips, and another color to be attracted to another series of strips. As such they were able to create a highly pixelated RGB LED device, which could in turn be used as either a PD device or an image sensor. This method would be highly effective, though it relies upon photolithography to pattern the electrodes.

A similar method has been used for LEDs using CdSe/CdS core/shell nanorods, similar in nature to QDs though they are longer in one dimension than in the others. Zhang et al. were able to use EPD to deposit a thin film of these nanorods onto an electrode of ZnO coated ITO. This has a lot of potential for many PDD devices as ZnO is one of the most commonly used ETL layers, for example, in thin film solar cells or even in LED devices as found here. It was also found that aligning these nanorods vertically improved the current density at higher voltages, which

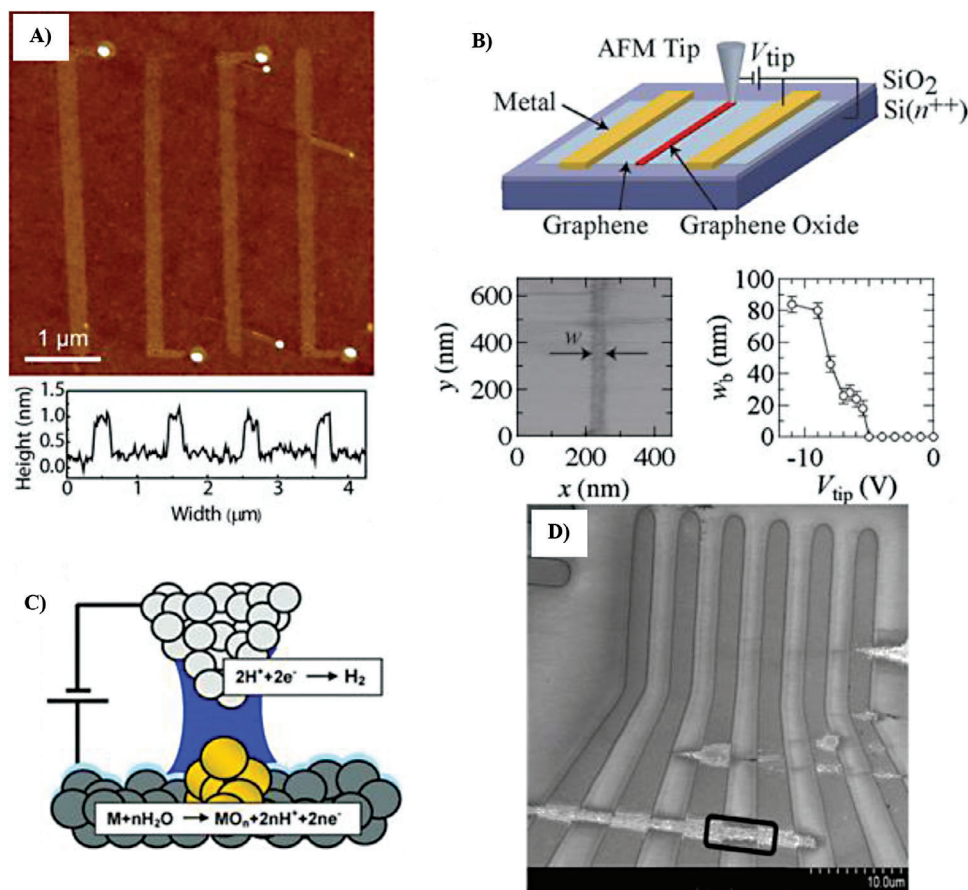


Figure 25. A) AFM image and height profile of rhodamine 6G attached to graphene by Zhou et al. Reproduced with permission,^[127] 2013, American Chemical Society. B) representation of the process of oxidizing a graphene electrode as carried out by Masubuchi et al. Reproduced with permission,^[130] 2011, American Chemical Society, and the corresponding friction image and a plot of the width of the line with the potential of the tip. C) A diagram of the process of SPL carried out by Reproduced with permission,^[129] 2006, Royal Society of Chemistry, with generic equations for oxidations of a metal surface. D) A SEM image of the silver trace carried out by Hung et al. Reproduced with permission,^[125] 2011, American Chemical Society.

could be controlled through the EPD process. By changing the ligand coverage and the length of the nanorod, it was possible to align them to be vertical when depositing on the electrode. This allowed for the deposition of a monolayer and a bilayer of these nanorods which would otherwise have been impossible through other solution processed methods.

Organics can also be used in EPD. Zhang et al.^[120] used EPD to deposit thin films of (Z)-3-(2-isocyano-2-(4-nitrophenyl)vinyl)-9-octyl-6-(pyridine-4-yl)-9H-carbazole (CzPy) with various different halides onto ITO.^[120] It was found initially that the adhesion of the organic onto the ITO was not good, though with the addition of the halides, this improved. The solvent used was Acetonitrile due to its polar aprotic nature. EPD of organics can get quite complicated quickly if the orientation of the molecule is important, this is due to the interaction of the various different orbitals and bonds with the electric field, which in larger organic molecules can be very complicated. It was possible to achieve a 100 nm thick film after just 30 s at 20 V.^[120] This demonstrates the ability of EPD to be a fast method for depositing as opposed to CVD or thermal evaporation which typically take times that are orders of magnitude longer.

EPD can also be used for patterning of devices as mentioned in Section 4.4.4. SPL is a form of electrochemical lithography that uses the methods of microscopy or scanning to pattern devices, most commonly with AFM though it can also be used with STM.^[61] This can be done through various different means, one of the most promising is through deposition of monolayers through the oxidation of substrates. Garcia et al.^[129] achieved the patterning of a Si substrate through the use of AFM, the technique demonstrated in Figure 25C. By applying a small amount of water to the AFM tip, a liquid bridge could be formed between the tip and the electrode surface whenever contact was made, allowing for a completed circuit, and by extension EPD. This liquid bridge allowed for the fabrication of SiO₂ dots of ≈ 20 nm size.^[129] Similarly, Masubuchi et al.^[130] achieved the patterning of graphene with a layer of graphene oxide through the use of AFM shown in Figure 25B. By using local anodic oxidation dragging the AFM tip across the graphene electrode surface a patterned electrode was fabricated.

Another method of SPL is to use an ink on the probe instead of water, to allow for more targeted deposition, EPD of materials that are not oxides. This is known as Dip-pen Scanning

Probe Lithography (D-SPL)^[61] and has been used to deposit both nanoparticles and organics as well as other materials. Kuljanishvili et al.^[128] used this process to modify carbon nanotubes that had been grown by CVD on a Si/SiO₂ substrate in the attempt to make single walled carbon nanotubes. This was achieved by using a catalyst, ferric nitrate nonahydrate mixed with ferric chloride hexahydrate, as a nanoparticle ink to write on the substrate. This method was also used by Zhou et al. to dope a graphene substrate with rhodamine 6G.^[127]

One of the more potentially useful applications of this method in terms of PD fabrication would be following the work of Hung et al.^[125] who deposited highly conductive silver patterns onto a Si/SiO₂ substrate seen in Figure 25D. Lines down to 500 nm width were deposited using a silver nanoparticle ink.^[125] This would be highly useful to apply to PD or image sensor fabrication, allowing for electrodes to be patterned through this means, as opposed to through the more conventional methods typically used. Through this method, the devices fabricated could also potentially be integrated into a greater Si based circuit device.

Whether the intention is to pattern the devices through depositing the electrodes with EPD or the active layers of the device, EPD can be applied to either aspect to achieve potentially high quality devices through a solution processed medium. If more examples of SPL and electrochemical patterning are required, the following reviews are of use.^[61,62]

8. Conclusion and the Future

Solution processed PDs and image sensors are becoming increasingly more prevalent and efficient, almost reaching the performance of more traditionally made PDs.^[2-4,12] There are many different methods of fabrication for these devices, some of which have been covered here, such as spin-coating, inkjet printing, dip coating, and EPD.^[11,13,14,18] Each of these methods has advantages and drawbacks, though through combining them there are seemingly limitless methods of fabrication.

The benefits of organic and QD-based PDs over conventional PDs are numerous. For one, solution processing allows far more flexibility in fabrication, though it is more difficult to optimize and reproduce. The color fidelity of not only organics but especially QDs allow for far more faithful representations of images, and the increased efficiency from these materials over conventional ones.^[2,4,11] However, the irregularities of the films are still detrimental to the device performance. As such there is a major focus on improving the charge transport of these devices.

Using a combination of different solution processed methods appears to be an interesting approach for fabrication of PD devices and ultimately image sensors. Combining EPD with more novel methods such as inkjet printing and dip coating would allow for far more intricate structures to be produced on a far larger scale. For example, managing to combine EPD with dip coating could allow for the deposition of multiple layers from one solution in one simple procedure, and then combining that with inkjet printed layers or electrodes would revolutionize how these devices are fabricated in industry.

When considering filter-less image sensors, the main aim for the future, OPDs, and QPDs represent one of the most promising ideas. The ability to manufacture large area flexible devices

using solution-processed methods is a large benefit of organics and QDs for this area in particular. This review has shown there are many promising areas for filter-less solution processed image sensors ranging from everyday use in cameras through to bioimaging.

Acknowledgements

The authors acknowledge the financial support from the EPSRC SWIMS (EP/V039717/1), the Leverhulme Trust (RPG-2022-263). W.S., P.M.S., and B.H. also acknowledge for the EPSRC for funding the PhD Studentship (EP/W524682/1: 2728029).

Conflict of Interest

There are no conflicts of interest.

Keywords

colloidal quantum dot, image sensor, organic semiconductor, patterning, photodetector

Received: April 21, 2024

Revised: August 19, 2024

Published online:

- [1] S. Al-Sarawi, M. Anbar, R. Abdullah, A. B. Al Hawari, presented at *2020 Fourth World Conf. on Smart Trends in Systems, Security and Sustainability (WorldS4)*, London, UK, July 2020, 449.
- [2] R. D. Jansen-Van Vuuren, A. Armin, A. K. Pandey, P. L. Burn, P. Meredith, *Adv. Mater.* **2016**, *28*, 4766.
- [3] H. Ren, J. D. Chen, Y. Q. Li, J. X. Tang, *Adv. Sci.* **2021**, *8*, 2002418.
- [4] R. Guo, M. Zhang, J. Ding, A. Liu, F. Huang, M. Sheng, *J. Mater. Chem. C Mater.* **2022**, *10*, 7404.
- [5] J. Ohta, *Smart CMOS Image Sensors and Applications*, CRC Press, Boca Raton **2020**
- [6] C. Y. Huang, A. H. Hu, J. Yin, H. C. Wang, *Int. J. Environ. Sci. Technol.* **2016**, *13*, 275.
- [7] M. Pelcat, GHG emissions of semiconductor manufacturing in 2021, <https://hal.science/hal-04112708v1> (accessed: July 2023).
- [8] F. Rasool, G. Wu, I. Shafiq, S. Kousar, S. Abid, N. Alhokbany, Ke Chen, *ACS Omega* **2023**, *9*, 3596
- [9] Y. K. Eom, S. H. Kang, I. T. Choi, Y. Yoo, J. Kim, H. K. Kim, *J. Mater. Chem. A Mater.* **2017**, *5*, 2297.
- [10] G. Ramalingam, P. Kathirgamanathan, G. Ravi, T. Elangovan, B. Arjun kumar, N. Manivannan, K. Kasinathan, *Quantum Confinement Effect of 2D Nanomaterials in Quantum Dots – Fundamental and Applications*, IntechOpen, London, UK **2020**
- [11] A. R. C. Osypiw, S. Lee, S.-M. Jung, S. Leoni, P. M. Smowton, B. Hou, J. M. Kim, G. A. J. Amaratunga, *Mater. Adv.* **2022**, *3*, 6773.
- [12] D. Natali, M. Caironi, *Photodetectors: Materials, Devices and Applications*, Woodhead, Cambridge, Cambridgeshire, UK **2016**, p. 195.
- [13] T. Shen, J. Yuan, X. Zhong, J. Tian, *J. Mater. Chem. C Mater.* **2019**, *7*, 6266.
- [14] C. Jiang, Z. Zhong, B. Liu, Z. He, J. Zou, L. Wang, J. Wang, J. Peng, Y. Cao, *ACS Appl. Mater. Interfaces* **2016**, *8*, 26162.
- [15] R. Eckstein, N. Strobel, T. Rödlmeier, K. Glaser, U. Lemmer, G. Hernandez-Sosa, *Adv. Opt. Mater.* **2018**, *6*, 1701108.
- [16] P. Kovacic, S. M. Willis, J. D. Matichak, H. E. Assender, A. A. R. Watt, *Org. Electron.* **2012**, *13*, 687.

- [17] D. M. Taylor, *Semicond. Sci. Technol.* **2015**, *30*, 054002.
- [18] J. Zhao, L. Chen, D. Li, Z. Shi, P. Liu, Z. Yao, H. Yang, T. Zou, B. Zhao, X. Zhang, H. Zhou, Y. Yang, W. Cao, X. Yan, S. Zhang, X. W. Sun, *Nat. Commun.* **2021**, *12*, 4603.
- [19] A. C. Poulouse, S. Veerananarayanan, S. H. Varghese, Y. Yoshida, T. Maekawa, D. Sakthi Kumar, *Chem. Phys. Lett.* **2012**, *539–540*, 197.
- [20] K. Rae, P. P. Manousiadis, M. S. Islim, L. Yin, J. Carreira, J. J. D. Mckendry, B. Guilhabert, I. D. W. Samuel, G. A. Turnbull, N. Laurand, H. Haas, M. D. Dawson, *Opt. Express* **2018**, *26*, 31474.
- [21] S. Y. Siew, B. Li, F. Gao, H. Y. Zheng, W. Zhang, P. Guo, S. W. Xie, A. Song, B. Dong, L. W. Luo, C. Li, X. Luo, G. Q. Lo, *J. Lightwave Technol.* **2021**, *39*, 4374.
- [22] C. Zeng, D. Fu, Y. Jin, Y. Han, *Photonics* **2023**, *10*, 573.
- [23] L. Sun, W. Li, W. Zhu, Z. Chen, *J. Mater. Chem. C Mater.* **2020**, *8*, 11664.
- [24] J. Liu, S. Bao, X. Wang, *Micromachines* **2022**, *13*, 184.
- [25] X. Li, C. Chen, Y. Yang, Z. Lei, H. Xu, *Adv. Sci.* **2020**, *7*, 2002320.
- [26] B. Ezhilmaran, A. Patra, S. Benny, S. M. R., A. V. V., S. V. Bhat, C. S. Rout, *J. Mater. Chem. C Mater.* **2021**, *9*, 6122.
- [27] U. Shafique, C. Santato, K. S. Karim, *IEEE Trans. Electron Devices* **2014**, *61*, 3465.
- [28] S. Y. Wang, S. D. Lin, H. W. Wu, C. P. Lee, *Appl. Phys. Lett.* **2001**, *78*, 1023.
- [29] Y. Li, H. Chen, J. Zhang, *Nanomaterials* **2021**, *11*, 1404.
- [30] A. Armin, R. D. Jansen-Van Vuuren, N. Kopidakis, P. L. Burn, P. Meredith, *Nat. Commun.* **2015**, *6*, 6343.
- [31] Z. Chen, Z. Cheng, J. Wang, X. Wan, C. Shu, H. K. Tsang, H. P. Ho, J.-B. Xu, *Adv. Opt. Mater.* **2015**, *3*, 1207.
- [32] K.-T. Lin, S.-C. Tseng, H.-L. Chen, Y.-S. Lai, S.-H. Chen, Y.-C. Tseng, T.-W. Chu, M.-Y. Lin, Y.-P. Lu, *J. Mater. Chem. C Mater.* **2013**, *1*, 4244.
- [33] Z. Lan, M.-H. Lee, F. Zhu, *Adv. Intell. Syst.* **2022**, *4*, 2100167.
- [34] M. Peng, Z. Wen, X. Sun, *Adv. Funct. Mater.* **2023**, *33*, 2211548.
- [35] P. C. Y. Chow, T. Someya, *Adv. Mater.* **2020**, *32*, 1902045.
- [36] X. Li, J. Wu, N. Mao, J. Zhang, Z. Lei, Z. Liu, H. Xu, *Carbon* **2015**, *92*, 126.
- [37] H. Lee, J. Ahn, S. Im, J. Kim, W. Choi, *Sci. Rep.* **2018**, *8*, 11545.
- [38] N. Hiromoto, T. Itabe, H. Shibai, H. Matsuhara, T. Nakagawa, H. Okuda, *Appl. Opt.* **1992**, *31*, 460.
- [39] G. Konstantatos, J. Clifford, L. Levina, E. H. Sargent, *Nat. Photonics* **2007**, *1*, 531.
- [40] G. Langfelder, A. Longoni, F. Zaraga, presented at *Sensors, 2009 IEEE*, Christchurch, New Zealand, October **2009**, 1652
- [41] M. Yamaguchi, H. Haneishi, N. Ohyama, *J. Imaging Sci. Techn.* **2008**, *52*, art00002.
- [42] R. J. Stover, M. Wei, Y. Lee, D. K. Gilmore, S. E. Holland, D. E. Groom, W. W. Moses, S. Perlmutter, G. Goldhaber, C. R. Pennypacker, N. W. Wang, N. P. Palaio, *Proc. SPIE 3505, Imaging System Technology for Remote Sensing*, Beijing, China, August **1998**.
- [43] J. Tiffenberg, M. Sofo-Haro, A. Drlica-Wagner, R. Essig, Y. Guardincerri, S. Holland, T. Volansky, T.-T. Yu, *Phys. Rev. Lett.* **2017**, *119*, 131802.
- [44] L. Jastrzebski, G. W. Cullen, W. N. Henry, S. Vecrumba, *J. Electrochem. Soc.* **1985**, *85–2*, 619.
- [45] M. El-Desouki, M. J. Deen, Q. Fang, L. Liu, F. Tse, D. Armstrong, *Sensors 2009* **2009**, *9*, 430.
- [46] M. Bigas, E. Cabruja, J. Forest, J. Salvi, *Microelectronics J.* **2006**, *37*, 433.
- [47] A. El Gamal, H. Eltoukhy, *IEEE Circuits and Devices Magazine* **2005**, *21*, 6.
- [48] D. H. Shin, S. H. Choi, *Coatings* **2018**, *8*, 329.
- [49] W. Bludau, A. Onton, W. Heinke, *J. Appl. Phys.* **1974**, *45*, 1846.
- [50] M. Yamazaki, S. Krishnadasan, A. J. Demello, J. C. Demello, *Lab Chip* **2012**, *12*, 4313.
- [51] D. M. Miller, N. M. Jokerst, S. Dhar, *Opt. Express* **2014**, *22*, 5052.
- [52] M. Marrs, E. Bawolek, J. T. Smith, G. B. Raupp, D. Morton, *SPIE - The Int. Society for Optical Engineering*, Vol. 8730, Flexible Electronics, Baltimore, MD, USA **2013**, pp. 28–34.
- [53] C. S. Schuster, B. R. Smith, B. J. Sanderson, J. T. Mullins, J. Atkins, P. Joshi, L. Mcnamara, T. F. Krauss, D. G. Jenkins, *Appl. Phys. Lett.* **2017**, *111*.
- [54] M. Zhou, Y.-P. Li, S. Zhou, D.-Q. Liu, *Chin. Phys. Lett.* **2015**, *32*, 077802.
- [55] M. Gulen, G. Yildirim, S. Bal, A. Varilci, I. Belenli, M. Oz, *J. Mater. Sci.: Mater. Electron.* **2013**, *24*, 467.
- [56] H. Shahariar, I. Kim, H. Soewardiman, J. S. Jur, *ACS Appl. Mater. Interfaces* **2019**, *13*, 6208.
- [57] C. J. Huang, Y. K. Su, S. L. Wu, *Mater. Chem. Phys.* **2004**, *84*, 146.
- [58] S. Y. Park, S. Lee, J. Yang, M. S. Kang, *Adv. Mater.* **2023**, *35*, 2300546.
- [59] Y. Chen, *Microelectron. Eng.* **2015**, *135*, 57.
- [60] A. Selimis, V. Mironov, M. Farsari, *Microelectron. Eng.* **2015**, *132*, 83.
- [61] P. Fan, J. Gao, H. Mao, Y. Geng, Y. Yan, Y. Wang, S. Goel, X. Luo, *Micromachines* **2022**, *13*, 228.
- [62] H. Liu, S. Hoepfener, U. S. Schubert, *Adv. Eng. Mater.* **2016**, *18*, 890.
- [63] T. C. Kuo, C. Y. Kuo, L. W. Chen, *Resour. Conserv. Recycl.* **2022**, *182*, 106289.
- [64] L. E. Manzer, *Science* **1990**, *249*, 31.
- [65] T. Kalsi, P. Kumar, *J. Phys. Chem. Solids* **2023**, *179*, 111377.
- [66] K. Nemoto, J. Watanabe, H. Yamada, H. T. Sun, N. Shirahata, *Nanoscale Adv.* **2023**, *5*, 907.
- [67] P. Giraud, B. Hou, S. Pak, J. I. Sohn, S. Morris, S. Cha, J. M. Kim, *Nanotechnology* **2018**, *29*, 075202.
- [68] G. Hu, L. Yang, Z. Yang, Y. Wang, X. Jin, J. Dai, Q. Wu, S. Liu, X. Zhu, X. Wang, T.-C. Wu, R. C. T. Howe, T. Albrow-Owen, L. W. T. Ng, Q. Yang, L. G. Occhipinti, R. I. Woodward, E. J. R. Kelleher, Z. Sun, X. Huang, M. Zhang, C. D. Bain, T. Hasan, *Sci. Adv.* **2020**, *6*.
- [69] P. Zhao, L. J. LeSergent, J. Farnese, J. Z. Wen, C. L. Ren, *Electrochem. Commun.* **2019**, *108*, 106558.
- [70] Y. Lei, J. Luo, X. Yang, T. Cai, R. Qi, L. Gu, Z. Zheng, *ACS Appl. Mater. Interfaces* **2020**, *12*, 24940.
- [71] C. Tan, M. Amani, C. Zhao, M. Hettick, X. Song, D.-H. Lien, H. Li, M. Yeh, V. R. Shrestha, K. B. Crozier, M. C. Scott, A. Javey, *Adv. Mater.* **2020**, *32*, 2001329.
- [72] H. Li, J. Huang, Q. Zheng, Y. Zheng, *Vacuum* **2020**, *172*, 109089.
- [73] S. K. Singh, P. Hazra, S. Tripathi, P. Chakrabarti, *Superlattices Microstruct.* **2016**, *91*, 62.
- [74] A. Yazmacyan, P. Meredith, A. Armin, *Adv. Opt. Mater.* **2019**, *7*, 1801543.
- [75] Z. Wang, Y. Wang, M. Liu, M. Xu, Z. Jiang, Y. Gao, H. Meng, X. Wang, *Adv. Opt. Mater.* **2023**, *11*, 2300493.
- [76] M. Liu, J. Wang, Z. Zhao, K. Yang, P. Durand, F. Ceugniet, G. Ulrich, L. Niu, Y. Ma, N. Leclerc, X. Ma, L. Shen, F. Zhang, *J. Phys. Chem. Lett.* **2021**, *12*, 2937.
- [77] H. M. Luong, S. Chae, A. Yi, K. Ding, J. Huang, B. M. Kim, C. Welton, J. Chen, H. Wakidi, Z. Du, H. J. Kim, H. Ade, G. N. M. Reddy, T.-Q. Nguyen, *ACS Energy Lett.* **2023**, *8*, 2130.
- [78] K. Pak, H. Seong, J. Choi, W. S. Hwang, S. G. Im, *Adv. Funct. Mater.* **2016**, *26*, 6574.
- [79] B. Hou, Y. Cho, B. S. Kim, J. Hong, J. B. Park, S. J. Ahn, J. I. Sohn, S. Cha, J. M. Kim, *ACS Energy Lett.* **2016**, *1*, 834.
- [80] U. Bothra, M. Albaladejo-Siguan, Y. Vaynzof, D. Kabra, *Adv. Opt. Mater.* **2023**, *11*, 2201897.
- [81] I. Moreels, K. Lambert, D. De Muynck, F. Vanhaecke, D. Poelman, J. C. Martins, G. Allan, Z. Hens, *Chem. Mater.* **2007**, *19*, 6101.
- [82] J. Sun, E. M. Goldys, *J. Phys. Chem. C* **2008**, *112*, 9261.
- [83] S. Pak, Y. Cho, J. Hong, J. Lee, S. Lee, B. Hou, G.-H. An, Y.-W. Lee, J. E. Jang, H. Im, S. M. Morris, J. I. Sohn, S. Cha, J. M. Kim, *ACS Appl. Mater. Interfaces* **2018**, *10*, 38264.
- [84] K. Jeong, J. Kim, M. G. Kang, *Sensors (Basel)* **2022**, *2981*, 22.

- [85] D. Knipp, P. G. Herzog, H. Stiebig, *IEEE Trans. Electron Devices* **2002**, 49, 170.
- [86] R. M. Turner, R. J. Guttosch, presented at *INICIS'06: International Congress of Imaging Science-Final Program and Proceedings*, Rochester, New York, May **2006**, 175.
- [87] A. Longoni, F. Zaraga, G. Langfelder, L. Bombelli, *IEEE Electron Device Lett.* **2008**, 29, 1306.
- [88] M. A. Martínez, E. M. Valero, J. Hernández-Andrés, J. Romero, G. Langfelder, *Appl. Opt.* **2014**, 53, C14.
- [89] J. Jiao, Y. Zhang, L. Shi, G. Li, T. Ji, W. Wang, R. Wen, Y. Hao, K. Wang, F. Zhu, Y. Cui, *Adv. Opt. Mater.* **2023**, 11, 2203132.
- [90] L. Peng, Y. Wang, Y. Ren, Z. Wang, P. Cao, G. Konstantatos, *ACS Nano* **2023**, 18, 5113.
- [91] J. Liu, P. Liu, D. Chen, T. Shi, X. Qu, L. Chen, T. Wu, J. Ke, K. Xiong, M. Li, H. Song, W. Wei, J. Cao, J. Zhang, L. Gao, J. Tang, *Nature Electronics* **2022**, 5, 443.
- [92] P. Peumans, A. Yakimov, S. R. Forrest, *J. Appl. Phys.* **2003**, 93, 3693.
- [93] B. Hou, B.-S. Kim, H. K. H. Lee, Y. Cho, P. Giraud, M. Liu, J. Zhang, M. L. Davies, J. R. Durrant, W. C. Tsoi, Z. Li, S. D. Dimitrov, J. I. Sohn, S. Cha, J. M. Kim, *Adv. Funct. Mater.* **2020**, 30, 2004563.
- [94] R. D. Jansen-Van Vuuren, P. C. Deakin, S. Olsen, P. L. Burn, *Dyes Pigm.* **2014**, 101, 1.
- [95] J. M. Lupton, R. Koeppel, J. G. Müller, J. Feldmann, U. Scherf, U. Lemmer, *Adv. Mater.* **2003**, 15, 1471.
- [96] B. Hou, D. Benito-Alifonso, R. F. Webster, D. Cherns, M. C. Galan, D. J. Fermín, *Catalysts* **2021**, 11, 681.
- [97] P. E. Keivanidis, P. K. H. Ho, R. H. Friend, N. C. Greenham, *Adv. Funct. Mater.* **2010**, 20, 3895.
- [98] F. Quinlan, T. M. Fortier, H. Jiang, A. Hati, C. Nelson, Y. Fu, J. C. Campbell, S. A. Diddams, *Nat. Photonics* **2013**, 7, 290.
- [99] T. Martin, R. Landauer, *Phys. Rev. B* **1992**, 45, 1742.
- [100] E. L. Dereniak, G. D. Boreman, (ed. D Glenn.). *Infrared detectors and systems*. Vol. 561, Wiley, Hoboken, New Jersey **1996**.
- [101] F. Guo, B. Yang, Y. Yuan, Z. Xiao, Q. Dong, Y. Bi, J. Huang, *Nat. Nanotechnol.* **2012**, 7, 798.
- [102] Z. Liu, K. Parvez, R. Li, R. Dong, X. Feng, K. Müllen, *Adv. Mater.* **2015**, 27, 669.
- [103] X. Gong, M. Tong, Y. Xia, W. Cai, J. S. Moon, Y. Cao, G. Yu, C.-L. Shieh, B. Nilsson, A. J. Heeger, *Science* **2009**, 325, 1665.
- [104] J. Lee, P. Jadhav, M. A. Baldo, *Appl. Phys. Lett.* **2009**, 95.
- [105] F. Guo, Z. Xiao, J. Huang, *Adv. Opt. Mater.* **2013**, 1, 289.
- [106] Y. Fang, F. Guo, Z. Xiao, J. Huang, *Adv. Opt. Mater.* **2014**, 2, 348.
- [107] H. Jin, A. Armin, M. Hamsch, Q. Lin, P. L. Burn, P. Meredith, *physica status solidi* **2015**, 212, 2246.
- [108] M. Stolterfoht, A. Armin, B. Philippa, R. D. White, P. L. Burn, P. Meredith, G. Juška, A. Pivrikas, *Sci. Rep.* **2015**, 5, 9949.
- [109] M. G. Bonomenna, *Smart Composite Coatings and Membranes: Transport, Structural, Environmental and Energy Applications*, Woodhead, Cambridge, Cambridgeshire **2016**, pp. 371–419.
- [110] E. Webster, *Print Unchained: Fifty Years of Digital Printing, 1950–2000 and Beyond: a Saga of Invention and Enterprise*, DRA of Vermont Inc, San Jose, California **2000**, 253.
- [111] N. Reis, C. Ainsley, B. Derby, *J. Appl. Phys.* **2005**, 97, 094903.
- [112] J. E. Fromm, *IBM J. Res. Dev.* **1984**, 28, 322.
- [113] A. Bard, L. Faulkner, *Electrochemical Methods: Fundamentals and Applications*, Wiley, Hoboken, New Jersey **2001**.
- [114] A. C. Fisher, *Electrode Dynamics*. Oxford University Press, **1996**.
- [115] F. Purcell-Milton, A. Curutchet, Y. Gun'ko, *Materials* **2019**, 12, 4089.
- [116] T. Li, W. Guo, L. Ma, W. Li, Z. Yu, Z. Han, S. Gao, L. Liu, D. Fan, Z. Wang, Y. Yang, W. Lin, Z. Luo, X. Chen, N. Dai, X. Tu, D. Pan, Y. Yao, P. Wang, Y. Nie, J. Wang, Y. Shi, X. Wang, *Nat. Nanotechnol.* **2021**, 16, 1201.
- [117] R. Walker, N. S. Holt, *Surface Technology* **1984**, 22, 165.
- [118] S. Bruckenstein, B. Miller, *Physicochemical Hydrodynamics* **1942**, 17, 115.
- [119] R. J. Forster, *Chem. Soc. Rev.* **1994**, 23, 289.
- [120] C. Zhang, H. Li, Y. Su, Q. Zhang, Y. Li, J. Lu, *ACS Appl. Mater. Interfaces* **2020**, 12, 15482.
- [121] T. Schmidt, E. Bauer, *Phys. Rev. B* **2000**, 62, 15815.
- [122] K. A. Lozovoy, A. G. Korotaev, A. P. Kokhanenko, V. V. Dirko, A. V. Voitsekhovskii, *Surf. Coat. Technol.* **2020**, 384, 125289.
- [123] A. Baskaran, P. Smereka, *J. Appl. Phys.* **2012**, 189, 111.
- [124] H. Z. Yu, C. V. Thompson, *Acta Mater.* **2014**, 67, 9672.
- [125] S.-C. Hung, O. A. Nafday, J. R. Haaheim, F. Ren, G. C. Chi, S. J. Pearton, *J. Phys. Chem. C* **2010**, 114, 145.
- [126] K. Salaita, Y. Wang, C. A. Mirkin, *Nat. Nanotechnol.* **2007**, 2, 1616.
- [127] X. Zhou, S. He, K. A. Brown, J. Mendez-Arroyo, F. Boey, C. A. Mirkin, *Nano Lett.* **2013**, 13, 2523.
- [128] I. Kuljanishvili, D. A. Dikin, S. Rozhok, S. Mayle, V. Chandrasekhar, *Small* **2009**, 5, 29.
- [129] R. Garcia, R. V. Martinez, J. Martinez, *Chem. Soc. Rev.* **2006**, 35, 4542.
- [130] S. Masubuchi, M. Arai, T. Machida, *Nano Lett.* **2011**, 11, 9405.
- [131] T. Talebi, B. Raissi, M. Haji, A. Maghsoudipour, *Int. J. Hydrogen Energy* **2010**, 35, 9405.
- [132] X. Gong, M. Tong, Y. Xia, W. Cai, J. S. Moon, Y. Cao, G. Yu, C.-L. Shieh, B. Nilsson, A. J. Heeger, A. C. Arias, *Science (1979)* **2009**, 325, 139.
- [133] I. Deckman, P. B. Lechêne, A. Pierre, A. C. Arias, *Org. Electron.* **2018**, 56, 5787.
- [134] C. Xu, P. Liu, C. Feng, Z. He, Y. Cao, *J. Mater. Chem. C Mater.* **2022**, 10, 5787.
- [135] J. Li, G. Liu, W. Liu, Y. Si, W. Deng, H. Wu, *Adv Photonics Res* **2022**, 3, 19182.
- [136] S. Suman, S. Dahiya, R. P. Jaiswal, P. Swaminathan, B. N. Pal, *J. Phys. Chem. C* **2023**, 127, 19182.
- [137] Y.-L. Wu, K. Fukuda, T. Yokota, T. Someya, *Adv. Mater.* **2019**, 31, 1903687.
- [138] T. Chen, S. Zhan, B. Li, B. Hou, H. Zhou, *Adv. Opt. Mater.* **2024**, 12, 2302451.
- [139] K. Qiao, H. Deng, X. Yang, D. Dong, M. Li, L. Hu, H. Liu, H. Song, J. Tang, *Nanoscale* **2016**, 8, 7137.
- [140] Z. Ma, J. Li, Y. Zhang, H. Zhao, Q. Li, C. Ma, J. Yao, *Nanotechnology* **2021**, 32, 12708.
- [141] T. Kalsi, P. Kumar, *Dalton Trans.* **2021**, 50, 16001.
- [142] S. Zhan, X.-B. Fan, J. Zhang, J. Yang, S. Y. Bang, S. D. Han, D.-W. Shin, S. Lee, H. W. Choi, X. Wang, B. Hou, L. G. Occhipinti, J. M. Kim, *J. Mater. Chem. C Mater.* **2020**, 8, 849.
- [143] J.-K. Song, J. Kim, J. Yoon, J. H. Koo, H. Jung, K. Kang, S.-H. Sunwoo, S. Yoo, H. Chang, J. Jo, W. Baek, S. Lee, M. Lee, H. J. Kim, M. Shin, Y. J. Yoo, Y. M. Song, T. Hyeon, D.-H. Kim, D. Son, *Nature Nanotechnology* **2022**, 17, 849.
- [144] A. B. Patel, P. Chauhan, H. K. Machhi, S. Narayan, C. K. Sumesh, K. D. Patel, S. S. Soni, P. K. Jha, G. K. Solanki, V. M. Pathak, *Phys. E Low Dimens. Syst. Nanostruct.* **2020**, 119, 1183.
- [145] M. N. Ishak, K. A. Yaacob, A. F. M. Noor, *J. Aust. Ceram. Soc.* **2022**, 58, 722.
- [146] P. K. Santra, P. V. Nair, K. George Thomas, P. V. Kamat, *J. Phys. Chem. Lett.* **2013**, 4, 2277.
- [147] B. Hou, F. C. Mocanu, Y. Cho, J. Lim, J. Feng, J. Zhang, J. Hong, S. Pak, J. B. Park, Y. W. Lee, J. Lee, B. S. Kim, S. M. Morris, J. I. Sohn, S. N. Cha, J. M. Kim, *Nano Lett.* **2023**, 23, 2277.
- [148] H. Zhang, R. Mao, L. Yuan, Y. Wang, W. Liu, J. Wang, H. Tai, Y. Jiang, *ACS Appl. Mater. Interfaces* **2024**, 16, 9088.
- [149] B. Xie, R. Xie, K. Zhang, Q. Yin, Z. Hu, G. Yu, F. Huang, Y. Cao, *Nat. Commun.* **2020**, 11, 2871.
- [150] H.-Y. Huang, J.-H. Chen, F. Nan, Y. Lin, L. Zhou, *Opt. Laser Technol.* **2023**, 166, 4298.
- [151] O. Atan, J. M. Pina, D. H. Parmar, P. Xia, Y. Zhang, A. Gulsaran, E. D. Jung, D. Choi, M. Imran, M. Yavuz, S. Hoogland, E. H. Sargent, *Nano Lett.* **2023**, 23, 25812.

- [152] W. Gong, P. Wang, W. Deng, X. Zhang, B. An, J. Li, Z. Sun, D. Dai, Z. Liu, J. Li, Y. Zhang, *ACS Appl. Mater. Interfaces* **2022**, *14*, 790.
- [153] C. Zhang, X. Yin, G. Chen, Z. Sang, Y. Yang, W. Que, *ACS Photonics* **2023**, *10*, 790.
- [154] Y. K. Ryu, R. Garcia, *Nanotechnology* **2017**, *28*, 142003.



William Solari is a second-year PhD student in Dr. Bo Hou's research group at Cardiff University. He earned his MPhys from the University of Bath's Department of Physics in 2022. William's research centers on the synthesis of colloidal quantum dots and the development of narrowband photodetectors using solution-processed techniques, with a particular focus on inkjet printing and electrochemistry.



Renjun Liu earned his master's degree in Microelectronics and Solid-State Electronics from Jilin University, followed by a PhD in Applied Physics and Materials Engineering from Macau University. He is currently a postdoctoral research associate in Dr. Bo Hou's group at Cardiff University, where his research focuses on the development of low-dimensional optoelectronic devices using advanced inkjet printing techniques.



Serena Nur Erkizan earned her B.S. degree in Physics from Middle East Technical University in 2019. For her M.S. studies, she explored the development of highly sensitive Surface Enhanced Raman Spectroscopy (SERS) substrates using femtosecond laser structuring and metal-assisted chemical etching. In 2023, Serena joined Dr. Bo Hou's research group at Cardiff University as a PhD student. Her current work focuses on Quantum dot-metal nanohybrids for Surface Enhanced Infrared Absorption Spectroscopy (SEIRA) and Quantum dot solar cells.



Bo Hou is a Senior Lecturer in the School of Physics and Astronomy at Cardiff University. He earned his PhD from the University of Bristol (2010–2014), followed by a postdoctoral research position at the University of Oxford (2014–2018, Wolfson College). He then served as a Senior Research Fellow at the University of Cambridge (2018–2020, St Edmund's College). Dr. Hou's research focuses on the synthesis of colloidal quantum dots (QDs), the development of QD solar cells and electronics, electron microscopy (TEM), and dynamic charge transfer analysis.